CrystEngComm

Crystal Engineering with 1,4-Piperazine-2,5-diones

Journal:	*CrystEngComm*
Manuscript ID:	CE-HIG-05-2014-000968.R1
Article Type:	Highlight
Date Submitted by the Author:	21-Jun-2014
Complete List of Authors:	Mash, Eugene; Universityof Arizona, Department of Chemistry

Crystal Engineering with 1,4-Piperazine-2,5-diones

Eugene A. Mash*

Abstract

Experimental testing of a paradigm for the design and construction of functional crystalline solids based on an indane/piperazinedione/indane scaffold is summarized. In theory, molecular assembly is predetermined by incorporation of chemically and geometrically orthogonal intermolecular interactions. Application of the paradigm to the development of materials possessing liquid crystalline and nonlinear optical properties is presented.

*Department of Chemistry and Biochemistry, University of Arizona, Tucson, AZ 85721-0041, USA. E-mail: emash@email.arizona.edu

1 Introduction

"Crystal engineering is the understanding of intermolecular interactions in the context of crystal packing and the utilization of such understanding in the design of new solids with desired physical and chemical properties." —from *Crystal Engineering a Textbook*[1]

Non-covalent interactions govern intermolecular contacts, which are of universal importance in chemistry, biology, and materials science. In their book *Supramolecular Chemistry*, Steed and Atwood list the following types of non-covalent interactions and their associated energies: ion-ion interactions (100-350 kJ/mol), ion-dipole interactions (50-200 kJ/mol), hydrogen bonding (4-120 kJ/mol), cation-π interactions (5-80 kJ/mol), dipole-dipole interactions (5-50 kJ/mol), π-π stacking (0-50 kJ/mol), and van der Waals forces (<5 kJ/mol).[2] Many early crystal engineering (CE) studies based on non-ionic, non-covalent interactions involved growth of crystals from mixtures containing two components expected to exhibit complementary interactions. This strategy, which we term co-crystal[3] engineering, has found application in the development of superior pharmaceutical agents.[4] Harnessing of the much stronger ionic interactions to drive component assembly led to the production of crystalline metal-organic frameworks,[5] often rigid, porous "host" materials useful in "guest" capture and storage, and in catalysis.[6] Other research has focused on what we term single-molecule crystal engineering and involves the design, synthesis, and crystallization of single molecules that, through the action of hydrogen bonding,[7] halogen bonding,[8] dipole-dipole interactions,[9] π-π stacking,[10] and/or van der Waals forces,[11] assemble spontaneously into solids, ideally with predictable packing and desirable bulk properties.[12-21] Our CE research falls into this latter category and has focused on molecules that contain 1,4-piperazine-2,5-dione rings. The crystal structure of the parent ring system was published in 1938,[22] and the solid-state structures and

bulk properties of "piperazinediones", also known as "diketopiperazines", have been of interest ever since.[23-46]

2 Assembly Paradigm

We postulated that the three-dimensional order in an organic crystal might be controlled by incorporation of three geometrically and chemically independent molecular recognition elements, represented by a three-color scheme in Figure 1.[47-49] To test this hypothesis, a family of piperazinedione-containing molecules **1**, derivable from substituted 2-aminoindan-2-carboxylic acids, was designed. The conformational freedom of such molecules is restricted,[50] limiting the number of possible packing options. At the same time, attachment of groups to the pentacyclic core can provide the necessary functional group variability with spatial control.

Regarding our expectations for crystal packing of compounds **1**, the hydrogen bonding properties of the piperazinedione ring were expected to play a central role in the establishment of order in the crystalline state. From a recent search of the Cambridge Structural Database (CSD), 156 nitrogen–unsubstituted, non–ionic piperazinediones were retrieved, 63% of which were found to form "one-dimensional" tapes[51] through reciprocal amide-to-amide $R_2^2(8)$ hydrogen bonding (along the A-axis, Figure 1).[52] Control of order in the second and third dimensions for hydrogen-bonded 1D tapes of **1** would then depend on harnessing arene-arene interactions (B-axis) and interactions due to the groups R^1 and R^2 (C-axis). Various arene interaction types have been recognized as important, from the packing of small molecules[53] to the stabilization of protein tertiary structures.[54] Parallel center-to-center association[55] is favored for arene rings that

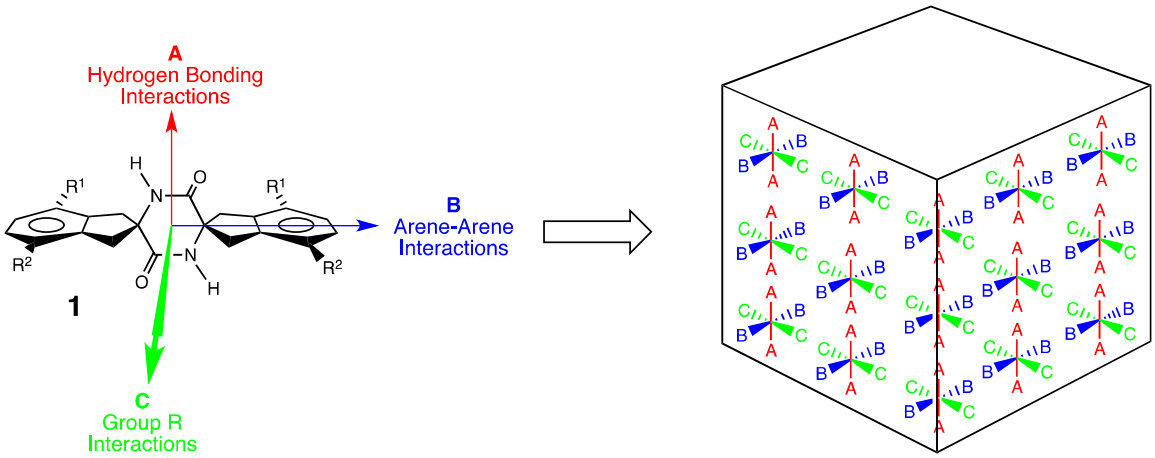

Figure 1. Piperazinedione scaffold **1** incorporating three geometrically and chemically independent recognition elements might assemble predictably into a solid.

possess very different electron densities, as in co-crystals of arenes and perfluoroarenes.[56-59] Parallel edge-to-center association[55] also is responsive to changes in π electron density due to substituent effects.[59-61] Perpendicular edge-to-center associations[55] are often observed for unsubstituted arenes, such as benzene, naphthalene, and anthracene.[62-64] The nature and magnitude of perpendicular edge-to-center associations have been subjected to much recent scrutiny.[65-72] What ever their cause, there appears to be agreement that such interactions are stabilizing, however weakly.

Logic would seem to dictate that for molecules with sufficiently large dipole moments, dipole-dipole interactions would play a role in determining crystal packing. However, a statistical analysis of crystallographic data[73,74] has frequently been cited as evidence that molecular dipole moments do not influence solid-state organization.[75] Other articles suggest that local dipoles due to functional groups may play a role if the dipoles are strong and in close proximity.[76] Dipoles may be aligned when topography requires alignment, as when "molecular egg cartons" are stacked upon each other,[77] or when the dipoles are well-separated by

containment in a host.[78] If the ordered packing of strong dipoles were easily accomplished, production of organic crystals that exhibit non-linear optic (NLO) properties would be straightforward. In fact, engineering such crystals has proven to be difficult. Nevertheless, a number of organic crystals possessing NLO properties due to at least a partial alignment of the chromophore-associated molecular dipoles have been described.[79]

van der Waals attractive interactions always contribute significantly to stabilization of the lattice as evidenced by the tendency of organic compounds to achieve closest packing in the solid state.[10,80] A number of publications on the development of porous solids with engineered cavities have appeared.[5,6,11,17,77,78,81] Invariably, the cavities are filled with guest molecules, often solvent, a further testament to the importance of van der Waals attractive interactions. Crystal engineers must therefore consider filling space sufficiently through shape complementarity when designing a crystal to be built from a single molecule.

3 Shape Complementarity, Thermochemistry, and Exhibition of Liquid Crystal Phases

Concomitant with our own early studies, Whitesides and co-workers examined the crystal packing of piperazinediones **2-9**.[23] In each case reciprocal amide-to-amide $R_2^2(8)$ hydrogen bonding afforded 1D tapes. Since **2-9** are symmetrical (no molecular dipole moments) and since the rings spirofused to the piperazinedione rings of **2-8** contain only non-polar hydrocarbon moieties, tape assembly in all directions perpendicular to the axis of hydrogen bonding depends on maximizing van der Waals contacts. For compounds **2** and **4-7**, this was achieved by adoption of planar piperazinedione ring conformations. The average planes of piperazinedione rings of adjacent molecules in each tape were parallel ($\tau_p = 0°$, see Table 1), and there were small ($\eta_p < 0.1$ Å) to modest ($0.1 < \eta_p < 0.4$ Å) progressive displacements of these average planes

along these tapes. For compounds **3**, **8**, and **9**, adoption of piperazinedione boat conformations, generating pairs of enantiomeric conformers, was observed. Tapes of **3** and **8** were composed of single enantiomeric conformers, adjacent tapes being enantiomeric, while tapes of **9** contained alternating enantiomeric conformers, adjacent tapes being related by screw symmetry. The average planes of piperazinedione rings of adjacent molecules in each tape were again parallel (τ_p = 0°), with modest progressive displacements of these planes along tapes of **3** and **8** and quite a large alternating displacement (η_p = ±1.4 Å) along tapes of **9**. Although arene-arene interactions were discounted in the analysis of the crystal packing of **9**, arene alignment seems consistent with parallel edge-to-center association (vide infra). Interestingly, the lowest melting points were reported for compounds **3**, **8**, and **9** (Table 1). Assuming that hydrogen bonding is the strongest and most persistent of the intermolecular interactions, this fact seems inconsistent with the suggestion that compounds **3**, **8**, and **9** may possess stronger hydrogen bonding than the other compounds studied.

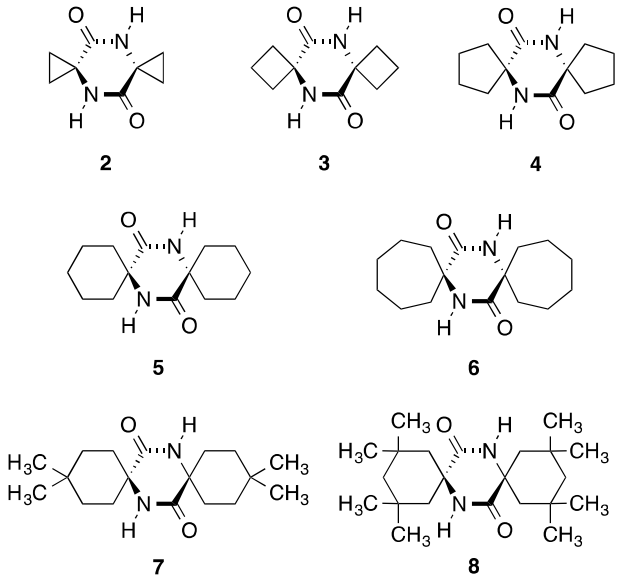

Table 1. Intermolecular Structural Parameters for Tape-forming Piperazinediones **2-16**, **20**, **22**, and **24-27**: Hydrogen Bonding.[a]

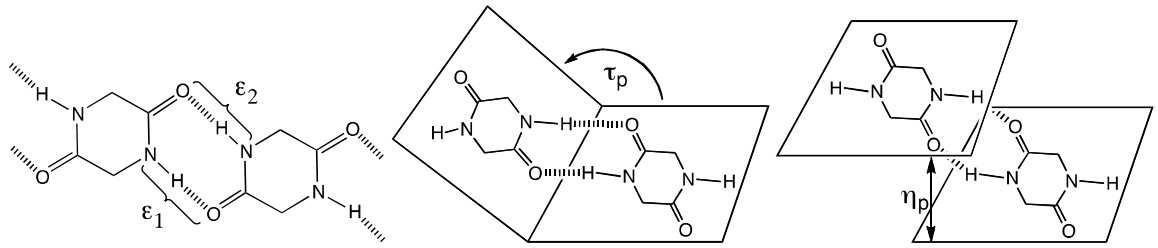

Compound	MP (°C)	N-O distances ε_1 (Å)[b]	N-O distances ε_2 (Å)[b]	τ_p (deg)[c]	η_p (Å)[d]	CSD □□□□□□□
2[e]	308	2.81		0.0	0.11	SIHVAG
3[e]	290	2.89	2.90	0.0	0.16	NUVZAF
4[e]	358	2.90		0.0	0.04	NUVYEI
5[e]	408-410	2.93		0.0	0.06	NUVYIM
6[e]	400	2.88		0.0	0.34	NUVYUY
7[e]	436	2.98		0.0	0.06	NUVYOS
8[e]	290	2.87	2.88	0.0	0.13	NUVZEJ
9[e]	297	2.88		0.0	1.45	NUVZIN
	322-324					NUVZIN01
10	>380 (dec)	2.85	2.86	0.0	0.04	EBOCED
11	311-312	2.87	2.87	0.0	0.12	EBOCON
12	344-346 (dec)	2.83	2.83	0.0	0.10	EBOCUT
13	>400	2.87		52.4	na[f]	EBOCAZ
14	316-318	2.80	2.94	69.2	na[f]	EBOCIH
		2.82	2.94			
15	317	2.84	2.84	0.0	0.23	CEWFER

16	293	2.80	2.80	0.0	0.40	CEWFIV
20[g]	180-182	2.88	2.88	0.0	0.37	VARPOU
20[h]		2.82	2.91	21.3	na[f]	
(*S,S*)-**22**[i]	360-362	2.84	2.86	0.0	0.07	EBOBOM
(*S,S*)-**22**[j]		2.85	2.82	0.0	0.20	
(*R,S*)-**22**	357-359	2.85	2.85	0.0	0.22	EBOBEC
(*S,S*)-**24**[k]	>300 (dec)[l]	2.98	3.03	0.0	0.14	MOKDOG
(*R,S*)-**24**	>300 (dec)	3.03	3.03	0.0	0.00	MOKFEY
(*S,S*)-**25**	302-308	2.85	2.87	0.0	0.34	EBOBAY
(*R,S*)-**25**	>290 (dec)	2.84	2.89	0.0	0.54	EBIZUK
(*S,S*)-**26**	310-312	2.84	2.86	0.0	0.44	ULEKIF
(*R,S*)-**26**	312-314	2.85	2.87	0.0	0.34	ULEKEB
(*S,S*)-**27**	>300 (dec)	2.84	2.85	0.0	00.54	MOLJUT
(*R,S*)-**27**	>280 (dec)	2.91	2.93	0.0	0.21	MOKFIC
CSD average	na[f]	2.89		0.0	nd[m]	

[a]Values are listed for each unique substructural component. [b]The distance between the amide nitrogen and oxygen atoms involved in hydrogen bonding. [c]The dihedral angle τ_p is formed by the intersection of the average planes defined by the atoms of piperazinedione rings adjacent in a tape. [d]The distance η_p lies between parallel average planes defined by the atoms of adjacent piperazinedione rings in a tape. [e]Data taken from reference 23. [f]Not applicable. [g]Interactions of conformers **20**A/**20**B with *ent*-**20**A/*ent*-**20**B. [h]Interactions of conformers **20**A/*ent*-**20**A and **20**B/*ent*-**20**B with **20**C/**20**D. [i]Interactions of conformer **22**A. [j]Interactions of conformer **22**B. [k]A 1:1 co-crystal with DMF. [l]Melting point of solvent-free material. [m]Not determined.

In addition to piperazinedione **9**, we studied the crystal packing of arene-substituted analogs **10-14**.[82] Like **2-8**, molecules **9-11** are achiral and have no molecular dipole moment, at least in solution. Molecules **12-14** are also achiral but are weakly dipolar.[83] Unlike **2-8**, compounds **9-14** might be expected to engage in arene interactions of one type or another. Thus, we looked for the possible participation of hydrogen bonding, arene, dipole, and van der Waals interactions in the analysis of the crystal packing of **9-14**.

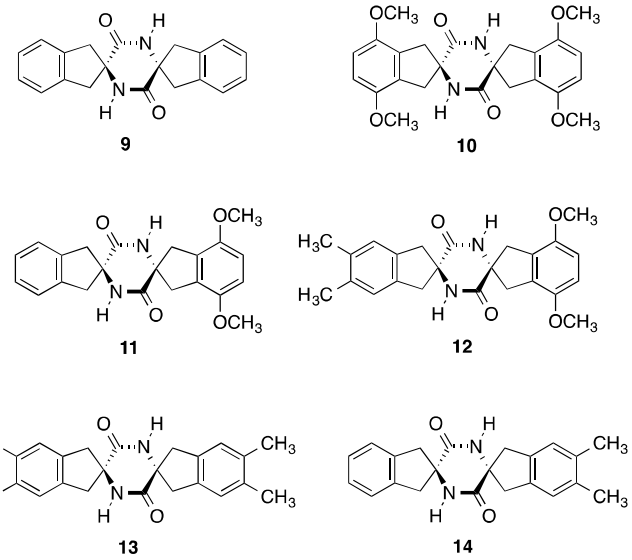

As was the case for compounds **2-8**, piperazinediones **9-14** exhibited reciprocal amide-to-amide $R_2^2(8)$ hydrogen bonding and afforded 1D tapes (see Table 1 and Figures 2-4). However, the molecular conformations and tape constructions were more varied. In crystals of **9-14**, no piperazinedione ring was truly flat. Crystals of compound **13** contained a single, very shallow chair conformation that possessed a center of inversion. Crystals of compounds **10** and **11** contained single conformational enantiomers present in boat and twist-boat conformations, respectively. Crystals of compounds **9** and **12** contained pairs of conformational enantiomers present in boat and twist-boat conformations, respectively. Crystals of compound **14** contained two pairs of conformational enantiomers present in pseudo-half-chair conformations. Despite

this conformational diversity, the N–O distances ε_1 and ε_2, representative of the hydrogen bonding of neighboring molecules in a tape, were all very near to 2.89 Å, the CSD average (Table 1).

Invariably, the indane moieties of **9-14** were folded along the "cyclopentene hinges" toward the proximal piperazinedione nitrogen and away from the carbonyl. The least folding was observed for compound **9**, where the tapes consisted of alternating enantiomeric conformers, producing a "butterfly" motif seen when a 1D tape is viewed down the axis of hydrogen bonding (Figure 2, top). This tape motif permitted the pair-wise parallel edge-to-center association of arenes of "lateral neighbor tapes" (LNTs, defined using the directionality of the figure as the frame of reference), producing a dimpled 2D sheet. Nesting of the dimpled sheets to maximize van der Waals contacts completed the 3D assembly.

While the N–O distances ε_1 and ε_2 for **10-12** were very near to the CSD average, the presence of methoxy substituents at positions 4 and 7 on one or both of the indane rings produced very different crystal packing for these compounds. The symmetrically substituted tetramethoxy piperazinedione **10** exhibited a "bent H" motif when a 1D tape was viewed down the axis of hydrogen bonding (Figure 2, top), while tapes of **11** and **12** exhibited "bent T" motifs (Figure 3, top). For **10**, LNTs were related by screw symmetry, which resulted in herringbone alignments of neighboring arene rings (Figure 2, middle). Perpendicular edge-to-center arene–arene interactions occured on one tape edge, while "slipped" perpendicular edge-to-center interactions (involving a hydrogen of a methoxy group on one arene and the arene ring of a molecule in the LNT) occured on the other tape edge. For **11**, LNTs were related by screw symmetry and were arranged in a "head-to-head, tail-to-tail fashion" with molecular (and tape) dipoles opposed. Herringbone alignment enabled perpendicular edge-to-center arene–arene

interactions on both tape edges between like-substituted arene rings. For **12**, LNTs were also arranged in a "head-to-head, tail-to-tail fashion" with molecular (and tape) dipoles opposed. "Slipped" perpendicular edge-to-center interactions occured between methoxy-substituted arenes, while van der Waals interactions were developed by shallow interdigitation of the methyl groups on the other tape edge, where parallel alignment of the arenes did not involve arene–arene interactions. The sheets of **10-12** possessed self-complementary topographies, and completed the 3D assemblies by stacking to maximize van der Waals contacts.

The N–O distances ε_1 and ε_2 for **13** and **14** were also near the CSD average, but the 1D tapes of these compounds were unusual in that the average planes of adjacent piperazinedione rings were significantly rotated, clockwise then counterclockwise, with respect to the axis of hydrogen bonding (τ_{pip} = 52° and 69° for **13** and **14**, respectively, Table 1). Tapes of **13** and **14** presented "bow tie" and "half bow tie" motifs in cross section when viewed down the axes of hydrogen bonding (Figure 4, top). The LNTs of **13** and **14** were vertically offset by half a period, while "vertical neighbor tapes" (VNTs, defined using the directionality of the figure as the frame of reference) were stacked in register. For **13**, this maximized the van der Waals interactions of the methyl groups at positions 5 and 6 (indane numbering), the presence of which precluded development of arene—arene interactions. For **14**, adjacent VNTs were enantiomeric, were stacked with the molecular (and tape) dipoles opposed, and developed perpendicular edge-to-center interactions between hydrogens of the unsubstituted arenes and the methyl-substituted arenes, as well as contacts between hydrogens of methyl substituents and unsubstituted arenes. Sheets of **14** comprised of VNTs assembled into 3D solids by shallow interdigitation of complementary surfaces (Figure 4). These results suggested that substitution at positions 5 and 6 should be avoided if development of arene—arene interactions is desired. A corollary, that

topographically complementary substitution at positions 5 and 6 may result in assembly through van der Waals-driven interdigitation of "notched" hydrogen-bonded tapes, is currently being tested (Figure 5).[84]

A line of investigation that was suggested by the crystal packing of **10** is schematically represented in Figure 6. If the methoxy substituents of **10** were replaced with longer normal alkoxy substituents in extended conformations, the H-shaped cross section of the reciprocally hydrogen bonded tape might be retained. This could permit the development of perpendicular edge-to-center arene–arene interactions as in the crystal of **10**, and possibly the bundling of alkyl tails in a manner that would foster their interdigitation. Compounds **15-21** were prepared to test this hypothesis.[85]

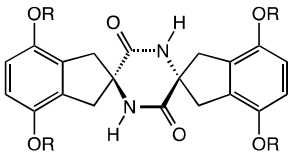

10 R = CH_3
15 R = CH_2CH_3
16 R = $(CH_2)_3CH_3$
17 R = $(CH_2)_5CH_3$
18 R = $(CH_2)_7CH_3$
19 R = $(CH_2)_8CH_3$
20 R = $(CH_2)_{11}CH_3$
21 R = $(CH_2)_{17}CH_3$

Although crystals of compounds **15-21** were obtained, to date only **15**, **16**, and **20** have yielded to single crystal X-ray analysis. The crystal packing of these compounds was remarkably similar to the packing of **10**. 1D tapes resulting from amide-to-amide $R_2^2(8)$ hydrogen bonding were observed in each case, and the N–O distances ε_1 and ε_2 were very near to the CSD average (see Table 1 and Figures 7 and 8). For **15** and **16**, hydrogen-bonded tapes contained a single enantiomeric conformation possessing C_i symmetry. LNTs were related by screw symmetry, producing herringbone packing motifs (Figure 7, middle). Perpendicular edge-to-center arene–arene interactions occured on both tape edges for **15**, while "slipped" perpendicular edge-to-center interactions (involving a hydrogen attached to C1 of the "kinked" butoxy group and an arene ring in the LNT) occurred on both tape edges for **16**. Given these observations and the

packing of **10**, it would appear that stabilization due to "slipped" perpendicular edge-to- center interactions involving a hydrogen attached to an sp^3 hybridized carbon is comparable to stabilization due to perpendicular edge-to-center arene-arene interactions involving a hydrogen attached to an sp^2 hybridized arene carbon and an adjacent arene π system.

The most complex of the piperazinedione crystal structures obtained was that of **20**.[86] Six conformations of the molecule, two pairs of enantiomeric conformers, **20A**, *ent*-**20A**, **20B**, and *ent*-**20B**, as well as two conformers with inversion symmetry, **20C** and **20D**, were present in the crystal in a 1:1:1:1:1:1 ratio (Figure 9). The piperazinedione rings of **20A**, *ent*-**20A**, **20B**, and *ent*-**20B** adopted unsymmetrical shallow boat conformations, while the piperazinedione rings of **20C** and **20D** were flat. In all cases, the cyclopentene subunits of the indane rings were substantially bent toward the nitrogen in the piperazinedione ring. While the dodecyloxy chains exhibited predominantly extended conformations, there were significant deviations from antiperiplanarity about several σ bonds in the chains. As a result, the dodecyloxy chains of **20A**, *ent*-**20A**, **20B**, and *ent*-**20B** projected away from the average planes defined by the arenes to which they were attached, while the dodecyloxy chains of **20C** and **20D** lay fairly close to these planes. Despite this conformational variability, molecules of **20** associated via reciprocal amide-to-amide $R_2^2(8)$ hydrogen bonding to form 1D-tapes with N–O distances ε_1 and ε_2 near the CSD average (Table 1 and Figure 8). LNTs associated, mostly through perpendicular edge-to-center arene interactions, but also through "slipped" perpendicular edge-to-center interactions, to give sheets very similar to those of the other tetraalkoxy piperazinediones studied. Furthermore, the dodecyloxy groups of **20** were deeply interdigitated in the space between the sheets defined by the pentacyclic cores, producing the 3D assembly observed in the crystal.

A plot of the observed freezing temperatures versus alkyl chain lengths for compounds **15-20** appears in Figure 10. It is noteworthy that the freezing temperatures decrease as the length of the alkoxy chains increase.[87] The available crystallographic data indicate that the geometries of the hydrogen bonds, and therefore their strengths, are very similar. If hydrogen bonds of comparable strength are the last intermolecular interactions broken during melting, and thus by the principle of microscopic reversibility the first intermolecular interactions formed during crystallization, the contribution of alkyl chain motion to the entropic component of the free energy could be responsible for the trend observed for the freezing temperatures. This issue is currently under investigation.[88]

Compounds **20** and **21** were of special interest in the context of possible liquid crystal properties.[89] Figure 11 presents the observed changes in layer spacing with temperature for **20** and **21** as determined by temperature-dependent X-ray analysis.[90] The changes in layer spacing appear to involve the dodecyloxy and octadecyloxy groups. Heating may cause these groups to become less entangled and more extended, making it possible for individual tapes or perhaps sets of LNTs to change register with respect to adjacent tapes or sheets. Similar movements should be possible in crystals of **10** and **15-19**, and DSC analyses suggest this may be the case.[85] Work is in progress with these compounds and with piperazinediones derived from 4,7-dialkyl-2-aminoindan-2-carboxylic acids to further test the assembly paradigm and to confirm its applicability to the design and production of compounds that display liquid crystal properties.

4 Chirality and the Pursuit of Dipole Alignment

Another motivation for our entry into the field of organic crystal engineering was the need to align dipolar chromophores in order to impart nonlinear optical properties to thermally stable bulk materials.[91] With respect to the latter issue, crystals of compounds **2-16** exhibited high melting temperatures (Table 1). We recognized that if the symmetry of piperazinedione **1** (Figure 1) was broken by incorporation of aligned dipolar chromophores in the arene rings, the molecule would be chiral.[92] We hoped that, with proper attention to other aspects of molecular design, we might develop a general method for dipole alignment in engineered high-melting crystals.[79]

We began our study with the production of sets of compounds **22-24** that exhibited a range of dipole moments,[93] but topographic features similar to each other and to the nonpolar, achiral piperazinedione **10**.[94] Solvent-free crystals of the *p*-bromoanisole derivatives (*S,S*)-**22** and (*R,S*)-**22** were grown from DMSO.[92,95] They exhibited molecular conformations and crystal packing similar to each other and to piperazinedione **10** (compare **10** in Figure 2 with (*S,S*)-**22** and (*R,S*)-**22** in Figure 12). In all three cases, reciprocal amide-to-amide $R_2^2(8)$ hydrogen bonding afforded tapes (see Table 1), and the "cyclopentene hinges" of the indane moieties were folded toward the piperazinedione nitrogen atoms, facilitating perpendicular edge-to-center arene assembly of LNTs and producing sheets that displayed herringbone packing motifs.

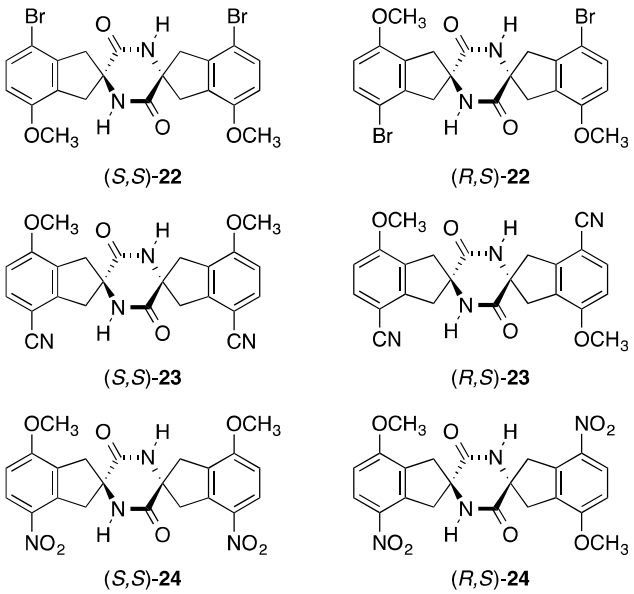

In the case of (*S,S*)-**22**, two conformers with nearly flat piperazinedione rings appeared in the crystal. Tapes were assembled, either from conformer (*S,S*)-**22**A (shown in blue) or (*S,S*)-**22**B (shown in green), and the conformer composition of LNTs alternated. Chirality required that the dipoles associated with the *p*-bromoanisole moieties be aligned in each tape. However, the herringbone assembly of LNTs placed the dipoles of perpendicular edge-to-center-associated arenes in opposition. The orientation of the dipoles with respect to VNTs was more complex—head-to-head, tail-to-tail, and head-to-tail pairings of closest neighbors were all observed (see Figure 12, bottom of left panel).

Crystals of (*R,S*)-**22** contained a single conformer with a flat piperazinedione ring. The crystallographic data supported random occupancy by the methoxy and bromine substituents at their positions in the unit cells. Given this fact and the similar packing of **10**, (*S,S*)-**22**, (*R,S*)-**22**, and the co-crystal of (*S,S*)-**22** and (*R,R*)-**22** (not shown),[95] it seemed reasonable to conclude that interactions between the *p*-bromoanisole dipoles did not play a significant role in crystal

assembly. Rather, the interplay between tape formation via hydrogen bonding, sheet formation via perpendicular edge-to-center arene association, and sheet assembly to give a solid with maximized van der Waals contacts was responsible for the outcome.

While we were able to grow crystals of the *p*-methoxybenzonitrile derivatives (*S,S*)-**23** and (*R,S*)-**23** from DMSO, solvent was invariably included.[96,97] Two DMSO molecules acted as hydrogen bond acceptors for the amide hydrogen bond donors, and a third disordered DMSO molecule filled space. This precluded tape formation by reciprocal amide-to-amide $R_2^2(8)$ hydrogen bonding, as well as comparisons of these crystal structures with those of compounds **10**, (*S,S*)-**22**, and (*R,S*)-**22**. Nevertheless, these crystals exhibited interesting features and properties. In the co-crystal of (*S,S*)-**23** with DMSO, a single pseudotwist-boat conformer was present in which the methoxy groups of the molecule were brought into closer proximity than the nitrile groups (Figure 13). The "cyclopentene hinges" of the indane moieties were folded only slightly toward the piperazinedione nitrogen atoms. Arene rings of neighboring molecules were arranged in a parallel edge-to-center fashion, and the *p*-methoxybenzonitrile dipoles were all reasonably well aligned. This collection of dipoles was opposed by the dipoles of the included DMSO molecules (not shown), which suggested that dipole compensation played a role in determining the crystal packing. The net dipole moment of the unit cell was estimated to be <1 D.[96] These co-crystals gave an NLO signal in the Kurtz and Perry powder test comparable to that of urea. Unfortunately, they began to melt when heated above 80 °C.

In an effort to exclude DMSO, (*S,S*)-**23** was crystalized from dipropylsulfoxide (DPSO).[96] This led to 1:2 co-crystals in which two DPSO molecules acted as the hydrogen bond acceptors for the amide hydrogen bond donors of (*S,S*)-**23**, while the hydrocarbon tails of the DPSO molecules acted as insulation. Two conformers of (*S,S*)-**23** were present in this co-crystal.

Both possessed pseudotwist-boat piperazinedione rings, one much flatter than the conformer seen in the co-crystal of (*S,S*)-**23** with DMSO, and the other as deeply puckered, but in the opposite direction, bringing the nitrile groups closer together than the methoxy groups (Figure 13). For the first time, the "cyclopentene hinges" of the indane moieties were folded, albeit slightly, toward the piperazinedione oxygen atoms. Arene rings of neighboring molecules were arranged in a parallel edge-to-center fashion, and again the *p*-methoxybenzonitrile dipoles were all reasonably well aligned; but in this co-crystal these dipoles were not opposed by the dipoles of the included DPSO molecules, which instead canceled each other. The net dipole moment of this unit cell was estimated to be >12 D.[97] These co-crystals began to melt when heated above 40 °C.

In the co-crystal of (*R,S*)-**23** with DMSO, a single conformer with a flat piperazinedione was present, and the "cyclopentene hinges" of the indane moieties were folded slightly toward the piperazinedione oxygen atoms (Figure 13). Arene rings of neighboring molecules were arranged in a parallel edge-to-center fashion, and the *p*-methoxybenzonitrile dipoles were opposed. These co-crystals decomposed when heated above 75 °C.

When freed of DMSO solvent in a DSC experiment or by column chromatography, amorphous (*S,S*)-**23** and (*R,S*)-**23** had melting points >300 °C, and (*S,S*)-**23** exhibited no NLO signal. These facts suggested that the solvent-containing co-crystals were the products of kinetically controlled crystallizations, and that antiparallel arrangement of the dipoles of (*S,S*)-**23** in the solid state was possible.

Crystals of the *p*-nitroanisole derivative (*S,S*)-**24** were grown from DMF, while crystals of (*R,S*)-**24** were grown from DMSO.[98,99] In the case of (*S,S*)-**24**, a single piperazinedione conformer containing a pseudotwist-boat was present, along with one disordered DMF molecule

that filled space. The cyclopentene subunits of the indane rings were nearly flat. Reciprocal amide-to-amide $R_2^2(8)$ hydrogen bonding produced tapes that exhibited a U-shaped motif when viewed along the axis of hydrogen bonding (Figure 14). LNTs were related by screw symmetry, leading to intercalation of the arene rings such that the dipoles of parallel edge-to-center associated *p*-nitroanisole moieties were opposed. Space between the methoxy substituents (i.e., the U-shaped groove of each tape) was filled with disordered DMF molecules, producing a 2D sheet with a shallow grooved topography. These sheets were stacked with the *p*-nitroanisole dipoles of VNTs in register in a head-to-tail alignment, presumably to maximize van der Waals contacts while developing energetically favorable dipole alignments (Figure 14).

In the crystal of (*R,S*)-**24**, a single conformer with flat piperazinedione and indane rings was present. Reciprocal amide-to-amide $R_2^2(8)$ hydrogen bonding produced tapes with dipoles aligned on each tape edge, but opposed on opposite edges of each tape (Figure 14). LNTs were related by screw symmetry, and parallel edge-to-center arene association resulted in opposition of proximal *p*-nitroanisole dipoles. The resulting corrugated sheets were stacked to maximize van der Waals contacts.

The question remained, could solvent-free crystals of (*S,S*)-**23** and (*S,S*)-**24**, if available, assemble in a manner similar to **10** and (*S,S*)-**22**? Insight can perhaps be obtained from comparisons of the crystal packing of compounds (*R,S*)-**25**, (*S,S*)-**26**, and (*S,S*)-**27**, prepared to prove the structures of the resolved amino acid precursors to **22-24**. An overlay of the crystal packing of these compounds is shown in Figure 15. These compounds exhibited similar conformations in their respective crystals, engaged in reciprocal amide-to-amide $R_2^2(8)$ hydrogen bonding to afford tapes, and possessed screw-related LNTs that engaged in herringbone packing, placing the dipoles of perpendicular edge-to-center-associated arenes in opposition. Sheet

assembly appeared to be governed by van der Waals complimentarity. While the diastereomers (*S,S*)-**25** and (*R,S*)-**26** packed in a very similar manner to that depicted in Figure 15, hydrogen-bonded and screw-related LNTs of (*R,S*)-**27** engaged in parallel edge-to-center arene interactions (not shown), much like (*S,S*)-**24** and (*R,S*)-**24**.

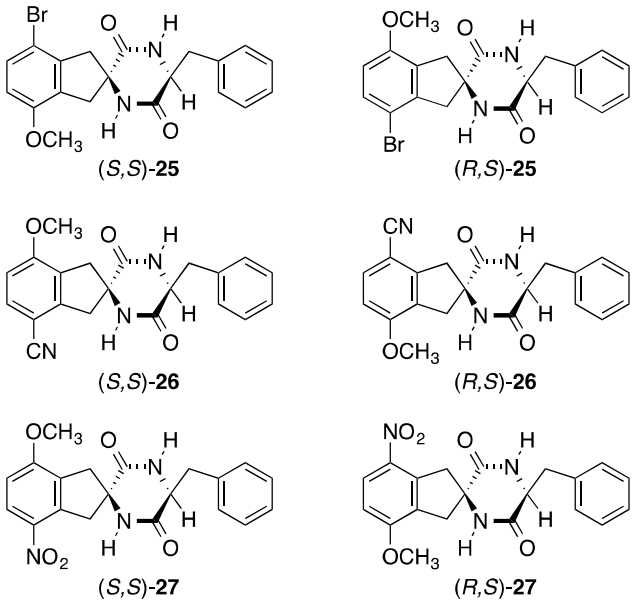

Studies with piperazinediones **22-27** suggest that, in the context of such molecular assemblies, arenes incorporating strong dipoles (3-6 D) favor parallel edge-to-center alignments, but can adopt perpendicular edge-to-center motifs; and that arene associations involving dipole opposition are favored, but not obligate.

5 Future Prospects

The piperazinedione-containing scaffold **1** has been a useful vehicle for testing our single-molecule crystal engineering assembly paradigm by the design and production of new liquid crystalline and non-linear optical materials. However, much potential for its use in the acquisition of new knowledge and the development of useful materials remains. For example,

starting from resolved (*S,S*)-**22**, modern methods for arene coupling are being used to extend the conjugation length and increase the dipole moment strength of possible NLO-active molecules. Additionally, we have prepared derivatives of the bis-amino acids **28-30** for production of molecules incorporating two or more piperazinedione rings.[100] Publications describing these advances will appear in due course.

(M)-**28**

(P)-**28**

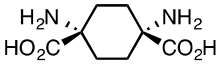

cis-**29**

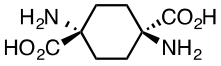

trans-**29**

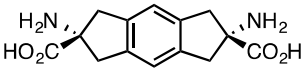

cis-**30**

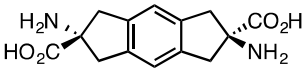

trans-**30**

Acknowledgment

The author is most grateful for the contributions of Lawrence J. Williams, Bhumasamudram Jagadish, Kirk E. Wells, Robin A. Weatherhead, Jeffrey R. Hammaker, Francis N. Murigi, Scott R. Lyon, and Pitambar Khanal. This work was supported in part by the Office of Naval Research through the Center for Advanced Multifunctional Nonlinear Optical Polymers and Molecular Assemblies, by the University of Arizona Office of the Vice President for Research, and by the Donors of the Petroleum Research Fund, administered by the American Chemical Society.

Notes and references

1. *Crystal Engineering A Textbook*, G. R. Desiraju, J. J. Vittal, and A. Ramanan; World Scientific Publishing Company: Singapore, 2011.

2. *Supramolecular Chemistry*, J. W. Steed and J. L. Atwood; John Wiley & Sons, Ltd: Chichester, United Kingdom, 2000.

3. For a discussion of the use of the term "co-crystal", see A. D. Bond, *CrystEngComm,* 2007, **9**, 833 and papers cited therein.

4. A. J. Florence, The Solid State, In *Modern Pharmaceutics*, 5th Ed.; A. T. Florence and J. Siepmann, Eds.; Informa Healthcare USA, Inc.: New York, 2009; Vol. 1, pp 253-310.

5. *Metal-Organic Frameworks: Design and Application*, L. R. MacGillivray, Ed.; John Wiley & Sons, Inc.: Hoboken, NJ, 2010.

6. *Metal-Organic Frameworks: Applications from Catalysis to Gas Storage*, D. Farrusseng, Ed.; John Wiley-VCH: Weinheim, Germany, 2011.

7. A. D. Burrows, Crystal Engineering Using Multiple Hydrogen Bonds, In *Structure and Bonding*; D. M. P. Mingos, Ed.; Springer-Verlag: Berlin, 2004; Vol. 108, pp 55-96.

8. F. Meyer and P. Dubois, *CrystEngComm,* 2013, **15**, 3058.

9. R. Paulini, K. Müller, and F. Diederich, *Angew. Chem. Int. Ed.,* 2005, **44**, 1788.

10. *The Importance of Pi-Interactions in Crystal Engineering: Frontiers in Crystal Engineering*, E. R. T. Tiekink and J. Zukerman-Schpector, Eds.; John Wiley & Sons, Ltd.: Chichester, United Kingdom, 2012.

11. Kitaigorodskii, A. I. *Molecular Crystals and Molecules*; Academic Press: New York, 1973.

12. J. D. Wuest, *Chem. Commun.,* 2005, 5830.

13. R. Glaser, *Acc. Chem. Res.,* 2007, **40**, 9.

14. C. Tschierske, *Chem. Soc. Rev.,* 2007, **36**, 1930.

15. R. Custelcean, *Chem. Commun.,* 2008, 295.

16. D. Braga, M. Curzi, S. L. Giaffreda, F. Grepioni, L. Maini, A. Pettersen, and M. Polito, Crystal Engineering with Ferrocene Compounds, In *Ferrocenes: Ligands, Materials, and Biomolecules*; P. Stepnicka, Ed.; John Wiley & Sons, Ltd.: Chichester, United Kingdom, 2008; Chapter 12, pp 465-498.

17. J. H. Chong and M. J. MacLachlan, *Chem. Soc. Rev.,* 2009, **38**, 3301.

18. R. Bishop, *Acc. Chem. Res.,* 2009, **42**, 67.

19. D. A. Hayes, *CrystEngComm,* 2011, **13**, 4793.

20. E. Cariati, G. Cavallo, A. Forni, G. Leem, P. Metrangolo, F. Meyer, T. Pilati, G. Resnati, S. Righetto, G. Terraneo, and E. Tordin, *Cryst. Growth Des.,* 2011, **11**, 5642.

21. J. C. Sumrak, A. N. Sokolov, and L. R. MacGillivray, Crystal Engineering Organic Semiconductors, In *Self-Organized Organic Semiconductors: From Materials to Device Applications*; Q. Li, Ed.; John Wiley & Sons, Inc.: Hoboken, NJ, 2011; Chapter 1, pp 1-19.

22. R. B. Corey, *J. Am. Chem. Soc.,* 1938, **60**, 1598.

23. M-J. Brienne, J. Gabard, M. Leclercq, J.-M. Lehn, M. Cesario, C. Pascard, M. Chevé, and G. Dutruc-Rosset, *Tetrahedron Lett.,* 1994, **35**, 8157.

24. S. Palacin, D. N. Chin, E. E. Simanek, J. C. MacDonald, G. M. Whitesides, M. T. McBride, and G. T. R. Palmore, *J. Am. Chem. Soc.,* 1997, **119**, 11807.

25. D. N. Chin, G. T. R. Palmore, and G. M. Whitesides, *J. Am. Chem. Soc.,* 1999, **121**, 2115.

26. G. T. R. Palmore, T.-J. M.. Luo, M. T. McBride-Wieser, E. A. Picciotto, and C. M. Reynoso-Paz, *Chem. Mater.,* 1999, **11**, 3315.

27. L. Ridvan, M. Budesínsky, M. Tichy, P. Malon, J. Závada, J. Podlaha, and I. Císarová, *Tetrahedron,* 1999, **55**, 12331.

28. W.-R. Li, K.-C. Kao, Y.-C. Yo, and C. K. Lai, *Helv. Chim. Acta,* 1999, **82**, 1400.

29. T-J. M. Luo and G. T. R. Palmore, *J. Phys. Org. Chem.,* 2000, **13**, 870.

30. T-J. M. Luo and G. T. R. Palmore, *Cryst. Growth Des.,* 2002, **2**, 337.

31. K. A. Lyssenko, D. A. Lenev, and R. G. Kostyanovsky, *Tetrahedron,* 2002, **58**, 8525.

32. C. G. Levins and C. E. Schafmeister, *J. Am. Chem. Soc.,* 2003, **125**, 4702.

33. K.-H. Park, M. M. Olmstead, and M. J. Kurth, *Synlett,* 2003, 1267.

34. D. A. Lenev, K. A. Lyssenko, and R. G. Kostyanovsky, *Mendelev Commun.,* 2004, **14**, 312.

35. S. W. Gordon-Wylie, E. Teplin, J. C. Morris, M. I. Trombley, S. M. McCarthy, W. M. Cleaver, and G. R. Clark, *Cryst. Growth Des.,* 2004, **4**, 789.

36. C. G. Levins and C. E. Schafmeister, *J. Org Chem.,* 2005, **70**, 9002.

37. T. R. Sarangarajan, B. S. Krishnamoorthy, K. Panchanatheswaran, J. N. Low, and C. Glidewell, *Acta Cryst.,* 2008, **C64**, m286.

38. C. E. Schafmeister, Z. Z. Brown, and S. Gupta, *Acc. Chem. Res.,* 2008, **41**, 1387.

39. S. Gupta and C. E. Schafmeister, *J. Org. Chem.,* 2009, **74**, 3652.

40. N. W. Polaske, G. S. Nichol, L. Z. Szabó, and B. Olenyuk, *Cryst. Growth Des.,* 2009, **9**, 2191.

41. Y. Ohta, K. Terada, T. Masuda, and F. Sanda, *Heterocycles,* 2009, **78**, 2523.

42. F. Blanco, I. Alkorta, I. Rozas, and J. Elguero, *J. Phys. Org. Chem.,* 2010, **23**, 1155.

43. Z. Z. Brown and C. E. Schafmeister, *Org. Lett.,* 2010, **12**, 1436.

44. T. Govindaraju, M. Pandeeswar, K. Jayaramulu, G. Jaipuria, and H. S. Atreya, *Supramol. Chem.,* 2011, **23**, 487.

45. Nonappa, K. Ahonen, M. Lahtinen, and E. Kolemainen, *Green Chem.,* 2011, **13**, 1203.

46. Z. Z. Brown, K. Akula, A. Arzumanyan, J. Alleva, M. Jackson, E. Bichenkov, J. B. Sheffield, M. A. Feitelson, and C. E. Schafmeister, *PLoS ONE* 2012, **7**, e45948.

47. S. R. Lyon, *Novel Materials for Photonic Applications,* Ph.D. Dissertation, The University of Arizona, Tucson, AZ, 1993.

48. L. J. Williams, *Design and Construction of Organic Crystals: Orthogonal Recognition of Piperazinediones Derived From Unnatural □-Amino Acids,* Ph.D. Dissertation, The University of Arizona, Tucson, AZ, 1996.

49. A formulation similar to this postulate has appeared in a review; see G. R. Desiraju, *Angew. Chem. Int. Ed.,* 2007, **46**, 8342.

50. The pentacyclic core of **1** is flexible about the cyclopentene "hinges" of the indane units and minimally flexible in the central piperazinedione ring. Although modeling indicates both rings prefer to be flat, each has been shown to adopt non-planar conformations to facilitate packing in the solid state.

51. We employ the term 'tape' as suggested by J. C. MacDonald and G. M. Whitesides, *Chem. Rev.,* 1994, **94**, 2383.

52. In May 2014, 156 nitrogen-unsubstituted non-ionic piperazinediones with 3D coordinates were retrieved from the Cambridge Structural Database (version 5.35, see F. H. Allen, *Acta Crystallogr. Sect. B,* 2002, **58**, 380); 63% possess one-dimensional "ladder-like" tapes (***i***), 4% form non-reciprocal hydrogen bonded networks (***ii***), and 33% develop alternate hydrogen bonded structures involving piperazinedione side chains and/or included molecules.

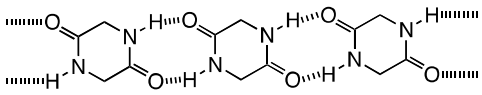

i

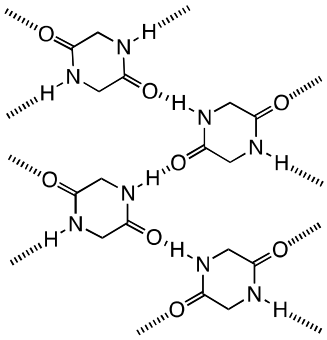

ii

53. C. A. Hunter, K. R. Lawson, J. Perkins, and C. J. Urch, *J. Chem. Soc., Perkin Trans. 2,* 2001, 651.

54. M. L. Waters, *Current Opinion in Chemical Biology,* 2002, **6**, 736.

55. The terms “parallel center-to-center”, “parallel edge-to-center”, and “perpendicular edge-to-center” will be used to describe arene interaction types herein. Other terms that have been used to designate arene interaction motifs include, for parallel center-to-center (***iii***), face-to-face, face-to-face stacked, parallel stacked, and stacked; for parallel edge-to-center (***iv***) face-to-face center-to-edge, parallel offset, offset stacked, and offset non-stacked; and for perpendicular edge-to-center (***v***) edge-to-face, edge-face, herringbone, and T-type.

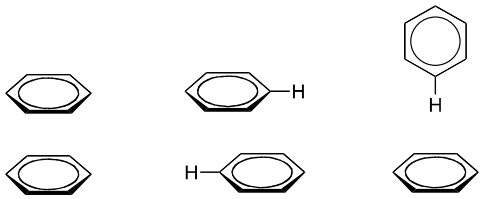

iii *iv* *v*

56. K. Reichenbächer, H. I. Süss, and J. Hulliger, *Chem. Soc. Rev.,* 2005, **34**, 22.

57. C. Dai, P. Nguyen, T. B. Marder, J. A. Scott, W. Clegg, and C. Viney, *J. Chem. Soc., Chem. Commun.,* 1999, 2493.

58. B. W. Gung, X. Xue, and Y. Zou, *J. Org. Chem.,* 2007, **72**, 2469.

59. W. R. Carroll, P. Pellechia, and K. D. Shimizu, *Org. Lett.,* 2008, **10**, 3547.

60. F. Cozzi, R. Annunziata, M. Benaglia, M. Cinquini, L. Raimondi, K. K. Baldridge, and J. S. Siegel, *Org. Biomol. Chem.,* 2003, **1**, 157.

61. B. W. Gung, X. Xue, and H. J. Reich, *J. Org. Chem.,* 2005, **70**, 3641.

62. A. Budzianowski and A. Katrusiak, *Acta Crystallogr., Sect. B,* 2006, **62**, 94, and prior structures for benzene.

63. J. Oddershede and S. Larsen, *J. Phys. Chem. A,* 2004, **108**, 1057, and prior structures for naphthalene.

64. B. Marciniak and V. Pavlyuk, *Mol. Cryst. Liq. Cryst. Sci. Technol., Sect. A,* 2002, **373**, 237, and prior structures for anthracene.

65. Y. Umezawa, S. Tsuboyama, K. Honda, J. Uzawa, and M. Nishio, *Bull. Chem. Soc. Jpn.,* 1998, **71**, 1207.

66. E. Kim, S. Paliwal, and C. S. Wilcox, *J. Am. Chem. Soc.,* 1998, **120**, 11192.

67. K. Nakamura and K. N. Houk, *Org. Lett.,* 1999, **1**, 2049.

68. J. Ribas, E. Cubero, F. J. Luque, and M. Orozco, *J. Org. Chem.,* 2002, **67**, 7057.

69. F. J. Carver, C. A. Hunter, D. J. Livingstone, J. F. McCabe, and E. M. Seward, *Chem. Eur. J.,* 2002, **8**, 2847.

70. S. L. Cockroft and C. A. Hunter, *Chem. Commun.,* 2006, 3806.

71. F. R. Fischer, W. B. Schweizer, and F. Diederich, *Chem. Commun.,* 2008, 4031.

72. A. K. Tewari and R. Dubey, *Bioorg. Med. Chem.,* 2008, **16**, 126.

73. J. K. Whitesell, R. E. Davis, L. L. Saunders, R. J. Wilson, and J. P. Feagins, *J. Am. Chem. Soc.,* 1991, **113**, 3267.

74. J. K. Whitesell, R. E. Davis, L. L. Saunders, R. J. Wilson, and J. P. Feagins, *J. Phys. D: Appl. Phys.,* 1993, **26**, B56.

75. A. Gavezzotti, *Acc. Chem. Res.,* 1994, **27**, 309.

76. S. Lee, A. B. Mallik, and D. C. Fredrickson, *Cryst. Growth Des.,* 2004, **4**, 279.

77. N. Malek, T. Maris, M.-É. Perron, and J. D. Wuest, *Angew. Chem. Int. Ed.,* 2005, **44**, 4021.

78. J. A. Swift and M. D. Ward, *Chem. Mater.,* 2000, **12**, 1501.

79. For a partial listing of crystals that exhibit NLO properties, see M. Jazbinsek and P. Günter, *Molecular Crystals and Crystalline Thin Films for Photonics*, in "Handbook of Organic Materials for Optical and (Opto)electronic Devices"; O. Ostroverkhova, Ed.; Woodhead Publishing: Oxford, 2013; Chapter 6.

80. L. E. Depero, *Adv. Mol. Struct. Res.,* 1995, **1**, 303.

81. C.-D. Wu, A. Hu, L. Zhang, and W. Lin, *J. Am. Chem. Soc.,* 2005, **127**, 8940.

82. L. J. Williams, B. Jagadish, S. R. Lyon, R. A. Kloster, M. D. Carducci, and E. A. Mash, *Tetrahedron,* 1999, **55**, 14281.

83. With the piperazinedione and indane rings constrained to be planar, the molecular dipole moments for **11**, **12**, and **14** were calculated to be 3.4, 3.0, and 0.4 D, respectively, using Spartan '10 for Macintosh.

84. F. N. Murigi, *Design, Synthesis, and Characterization of Indane 2,5–Diketopiperazines for Liquid Crystal Applications*, Ph.D. Dissertation, The University of Arizona, 2011.

85. K. E. Wells, R. A. Weatherhead, F. N. Murigi, G. S. Nichol, M. D. Carducci, H. D. Selby, and E. A. Mash, *Cryst. Growth . Des.,* 2012, **12**, 5056.

86. A more detailed analysis of the crystal packing of **20** appears in reference 85.

87. For a similar trend in the melting temperature of n-alkylammonium halides, see J. Tsau and D. F. R. Gilson, *J. Phys. Chem.,* 1968, **72**, 4082.

88. R. A. Weatherhead-Kloster, H. D. Selby, W. B. Miller III, and E. A. Mash, *J. Org. Chem.,* 2005, **70**, 8693.

89. R. A. Kloster, M. D. Carducci, and E. A. Mash, *Org. Lett.,* 2003, **5**, 3683.

90. N. A. Clark, D. M. Walba, and Y. Shen, personal communication of unpublished results.

91. F. Kajzar and J. Zyss, *Nonlinear Optics and Quantum Optics,* 2012, **43**, 31.

92. L. J. Williams, B. Jagadish, M. G. Lansdown, M. D. Carducci, and E. A. Mash, *Tetrahedron,* 1999, **55**, 14301.

93. Dipole moments of model compounds *vi*-*viii* were calculated at the semi-empirical AM1 level (equilibrium geometry) using Spartan '02 v1.0.4e.

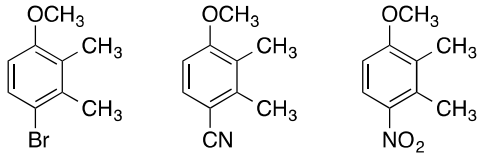

vi 1.78 D *vii* 3.32 D *viii* 5.99 D

94. Conformational energies (A values) indicate the nitro group (4.8 kJ/mol) is larger than nitrile (0.48 kJ/mol), bromine (ca 2.4 kJ/mol), or methoxy (ca 2.7 kJ/mol) groups. See E. L. Eliel, S. H. Wilen, and L. N. Mander, *Stereochemistry of Organic Compounds*; John Wiley & Sons: New York, 1994, p. 696 and references cited therein. Volume increments given for these groups are CN, 16 $Å^3$; Br, 26 $Å^3$; NO_2, 23 $Å^3$; and OMe, ca 30 $Å^3$. See ref 11, page 20.

95. In addition to (*S,S*)-**22** and (*R,S*)-**22**, crystals of a racemic mixture of (*S,S*)-**22** and (*R,R*)-**22** were also prepared and studied. Crystals of (*R,S*)-**22** and racemic **22** were nearly

isostructural and were indistinguishable by X-ray crystallography. See C. P. Brock and J. D. Dunitz, *Chem. Mater.,* 1994, **6**, 1118, footnote 57.

96. B. Jagadish, M. D. Carducci, C. Bosshard, P. Günter, J. I. Margolis, L. J. Williams, and E. A. Mash, *Cryst. Growth Des.,* 2003, **3**, 811.

97. In addition to (*S,S*)-**23** and (*R,S*)-**23**, crystals of a racemic mixture of (*S,S*)-**23** and (*R,R*)-**23** were also prepared and studied. A more complete description and analysis of the crystal packing of the co-crystals of (*S,S*)-**23**, (*R,S*)-**23**, and racemic **23** appears in reference 96.

98. D. Ntirampebura, B. Jagadish, G. S. Nichol, M. D. Carducci, A. Dawson, A. Rajapakshe, A. G. Oliver, W. Clegg, R. W. Harrington, L. Layne, Jr., J. I. Margolis, and E. A. Mash, *Cryst. Growth Des.,* 2008, **8**, 3257.

99. In addition to (*S,S*)-**24** and (*R,S*)-**24**, crystals of a racemic mixture of (*S,S*)-**24** and (*R,R*)-**24** were also prepared and studied. A more complete description and analysis of the crystal packing of the co-crystals of (*S,S*)-**24**, (*R,S*)-**24**, and racemic **24** appears in reference 98.

100. R. A. Weatherhead, M. D. Carducci, and E. A. Mash, *J. Org Chem.,* 2009, **74**, 8773.

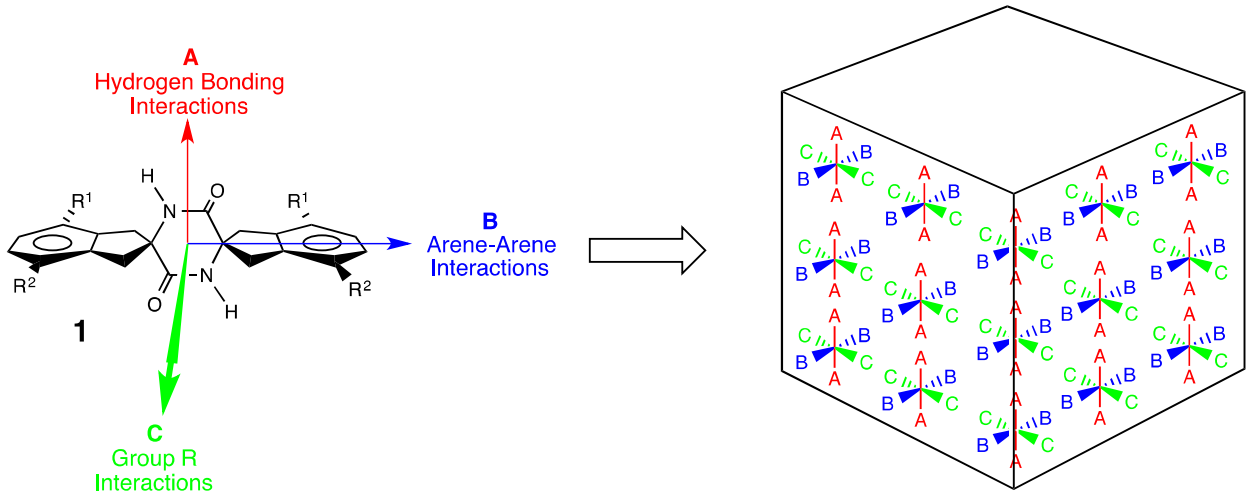

Figure 1. Piperazinedione scaffold **1** incorporating three geometrically and chemically independent recognition elements might assemble predictably into a solid.

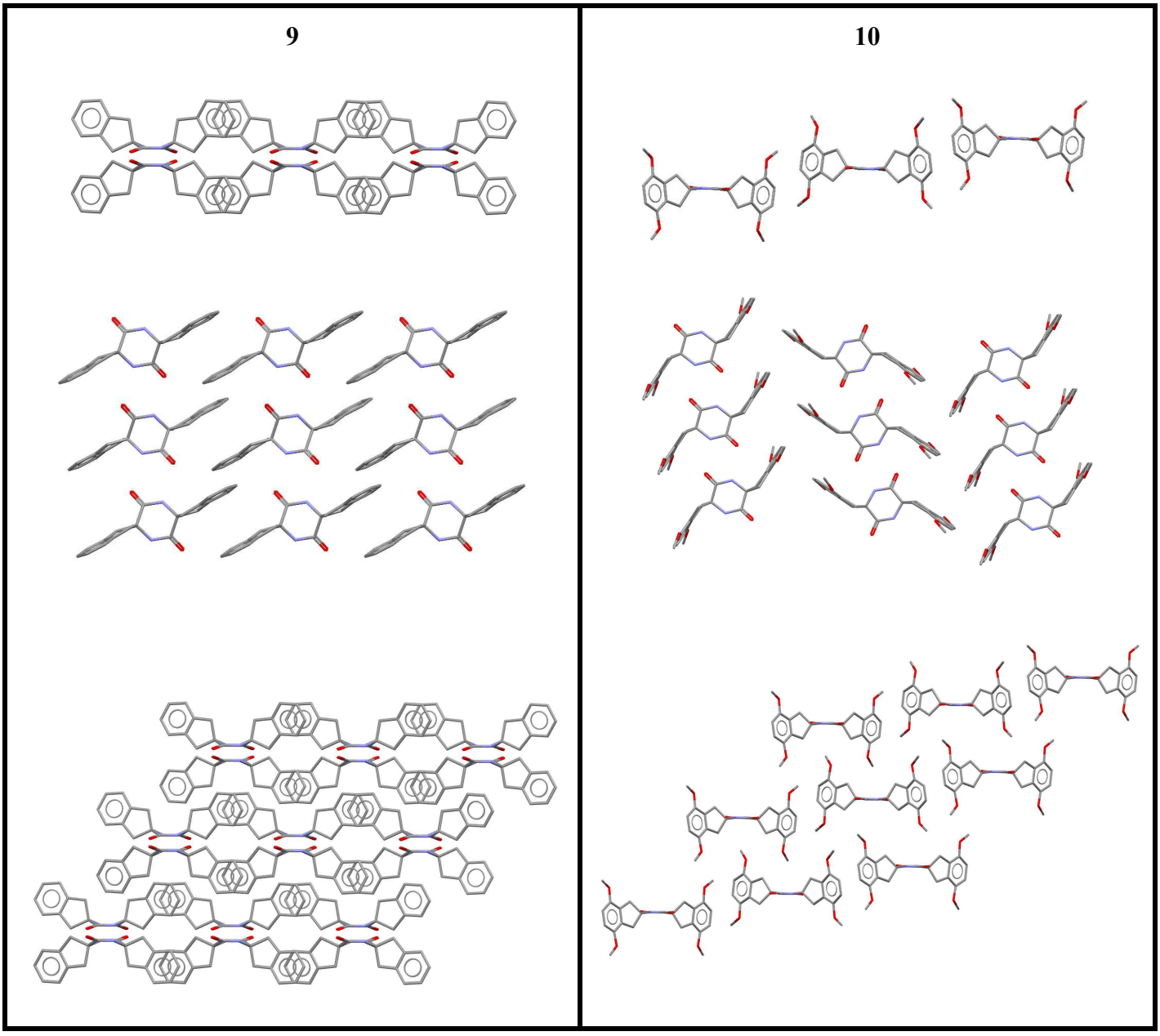

Figure 2. Crystal packing for piperazinediones **9** and **10**. Top of each panel: a view of a sheet (nine molecules) formed by three lateral neighbor tapes (LNTs) viewed down the hydrogen-bonding axis. Middle: a view of the sheet perpendicular to the hydrogen-bonding axis. Bottom: a view of three sheets (27 molecules) down the hydrogen-bonding axis. Hydrogen atoms are omitted for clarity. LNTs of **9** engage in parallel edge–to–center arene–arene interactions. LNTs of **10** engage in perpendicular edge–to–center interactions on one tape edge and in "slipped" perpendicular edge–to–center interactions on the other tape edge. Vertical neighbor tapes (VNTs) principally engage in van der Waals interactions through topographic complementarity.

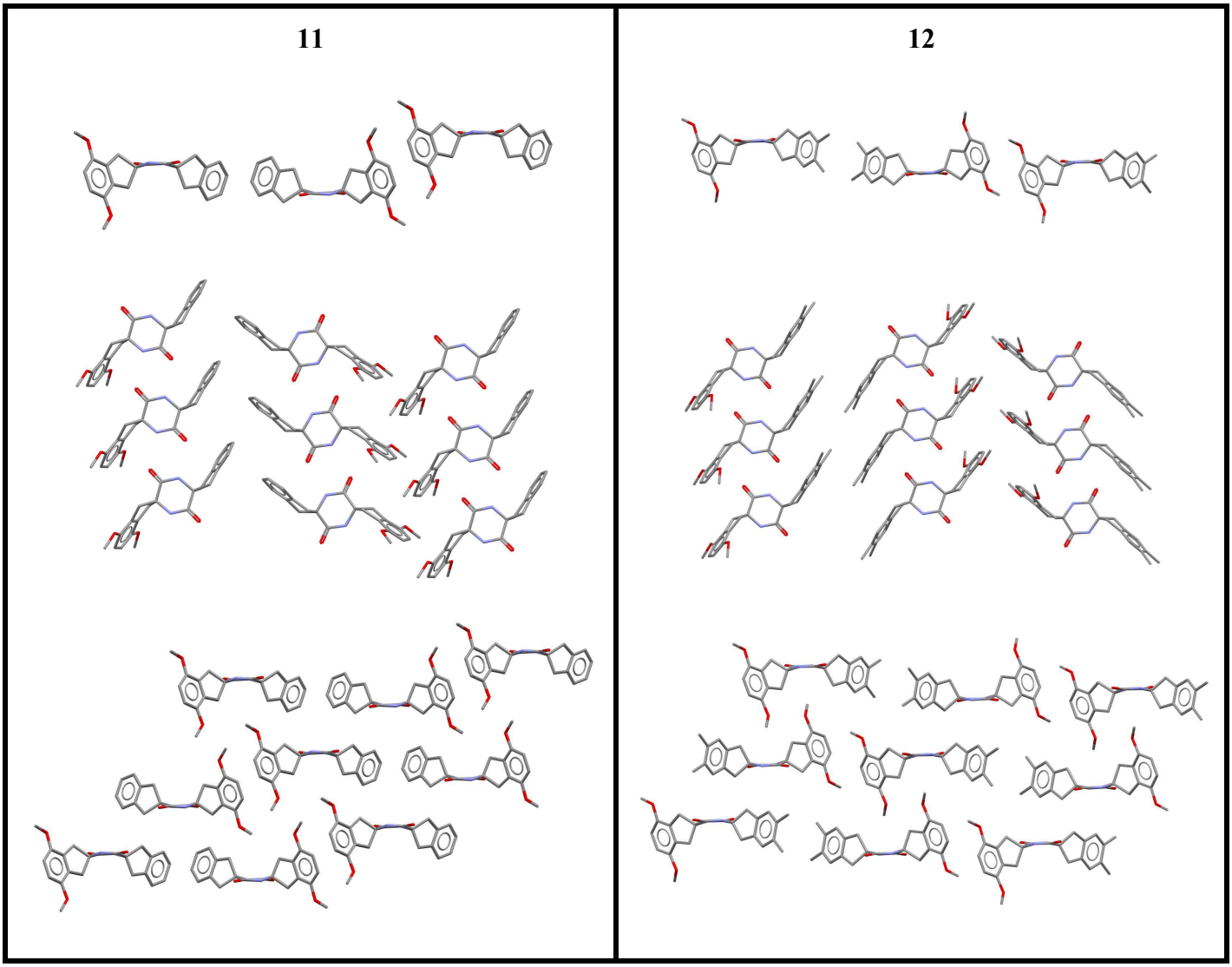

Figure 3. Crystal packing for piperazinediones **11** and **12**. Top of each panel: a view of a sheet (nine molecules) formed by three LNTs viewed down the hydrogen-bonding axis. Middle: a view of the sheet perpendicular to the hydrogen-bonding axis. Bottom: a view of three sheets (27 molecules) down the hydrogen-bonding axis. Hydrogen atoms are omitted for clarity. LNTs of **11** engage in perpendicular edge–to–center interactions on both tape edges. LNTs of **12** engage in "slipped" perpendicular edge–to–center interactions on one tape edge and in van der Waals interactions through topographic complementarity on the other tape edge. Vertical neighbor tapes (VNTs) principally engage in van der Waals interactions through topographic complementarity.

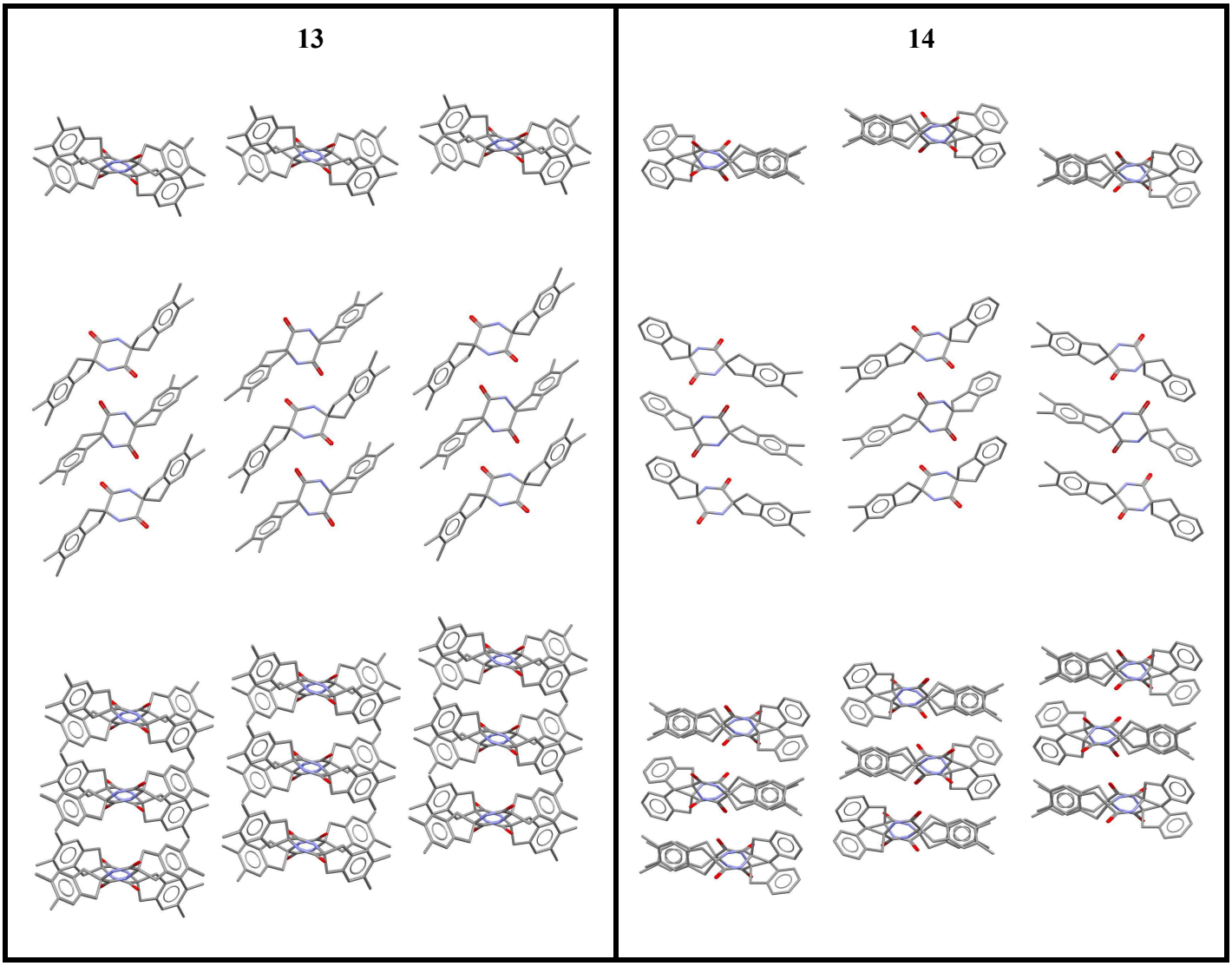

Figure 4. Crystal packing for piperazinediones **13** and **14**. Top of each panel: a view of a sheet (nine molecules) formed by three LNTs viewed down the hydrogen-bonding axis. Middle: a view of the sheet perpendicular to the hydrogen-bonding axis. Bottom: a view of three sheets (27 molecules) down the hydrogen-bonding axis. Hydrogen atoms are omitted for clarity. LNTs and VNTs of both **13** and **14** principally engage in van der Waals interactions through topographic complementarity.

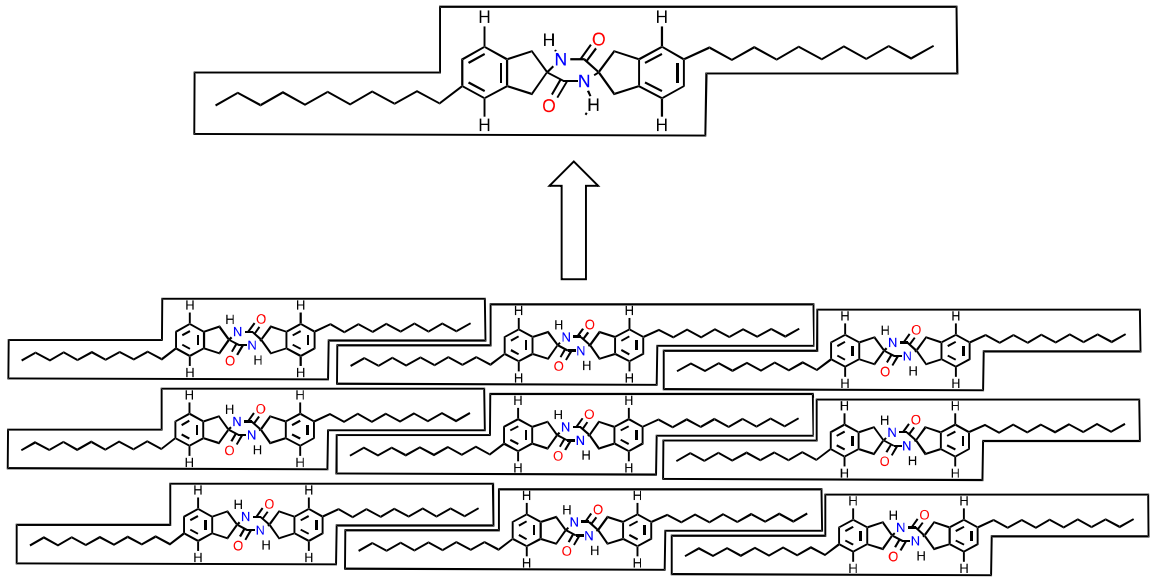

Figure 5. Schematic representations of a hypothetical hydrogen-bonded tape cross-section (top) and crystal packing (bottom) viewed parallel to the long axis of the tape.

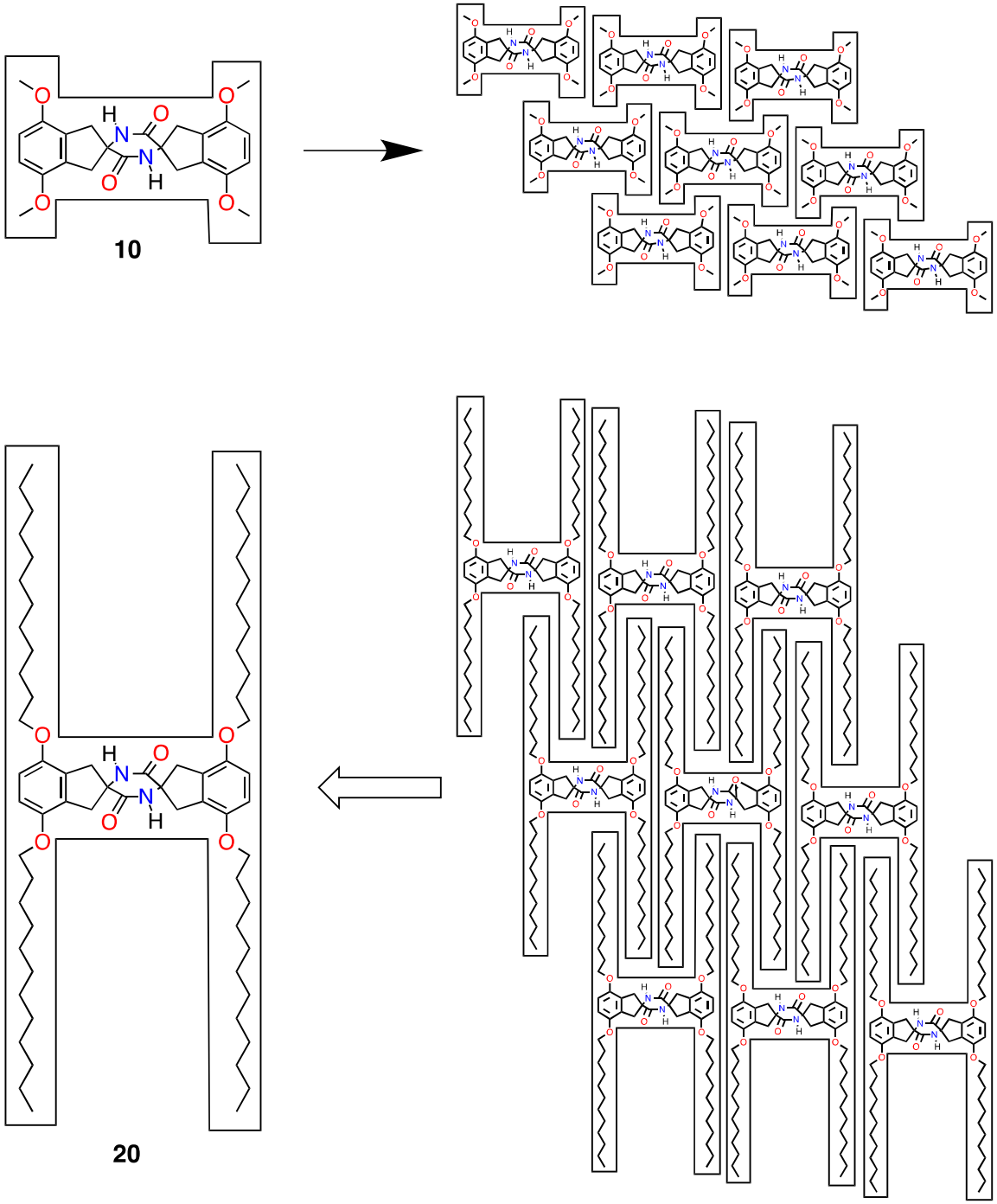

Figure 6. *Top:* Schematic representations of the hydrogen-bonded tape cross-section (left) and crystal packing (right) observed for compound **10**. *Bottom:* Schematic representations of a hypothetical hydrogen-bonded tape cross-section (left) and crystal packing (right) for **20**, the tetradodecyloxy homologue of compound **10**.

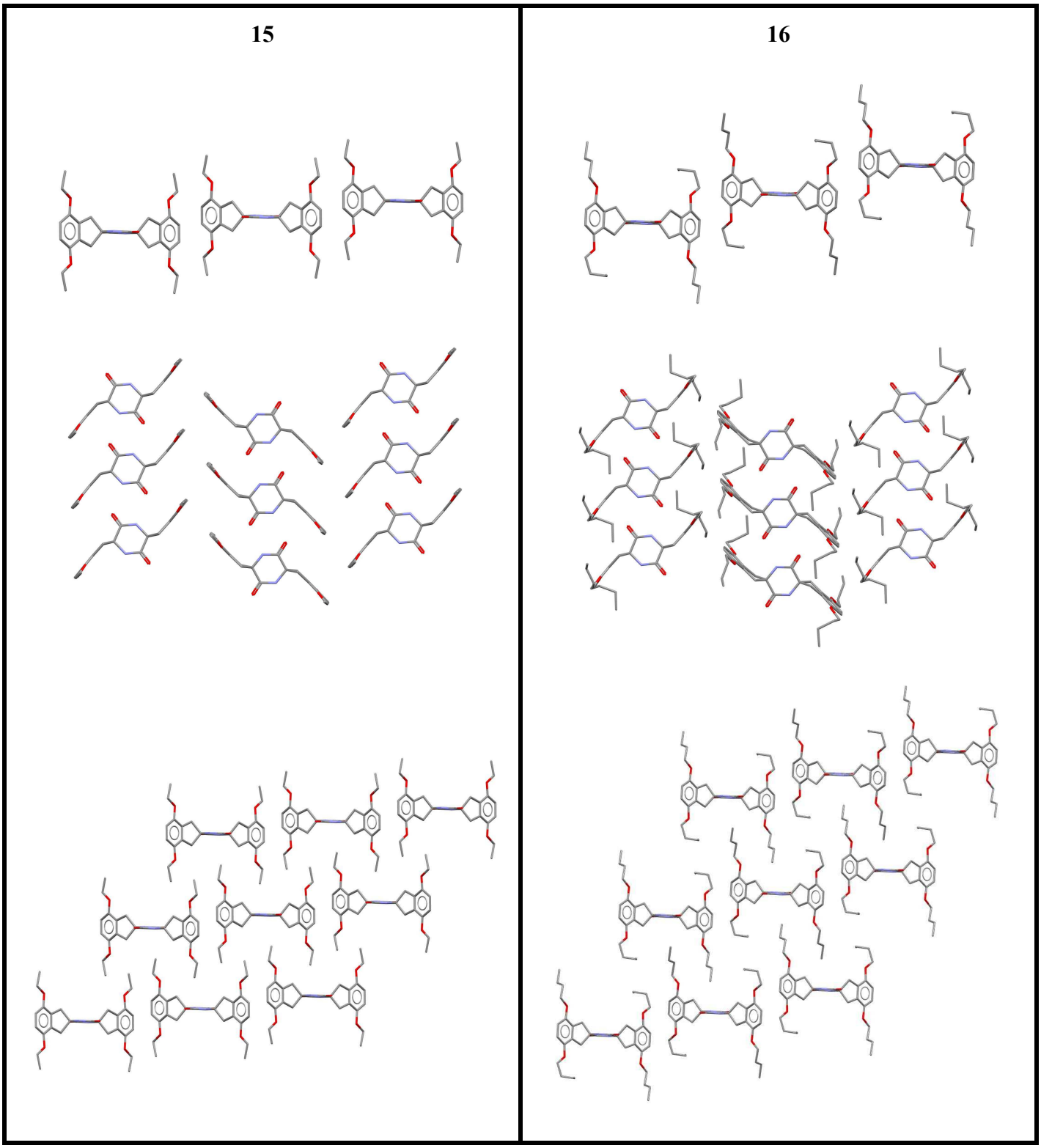

Figure 7. Crystal packing for piperazinediones **15** and **16**. Top of each panel: a view of a sheet (nine molecules) formed by three LNTs viewed down the hydrogen-bonding axis. Middle: a view of the sheet perpendicular to the hydrogen-bonding axis. Bottom: a view of three sheets (27 molecules) down the hydrogen-bonding axis. Hydrogen atoms are omitted for clarity. LNTs of **15** engage in perpendicular edge–to–center interactions, while LNTs of **16** engage in "slipped" perpendicular edge–to–center

interactions. VNTs engage in van der Waals interactions through topographic complementarity (interdigitation of tails).

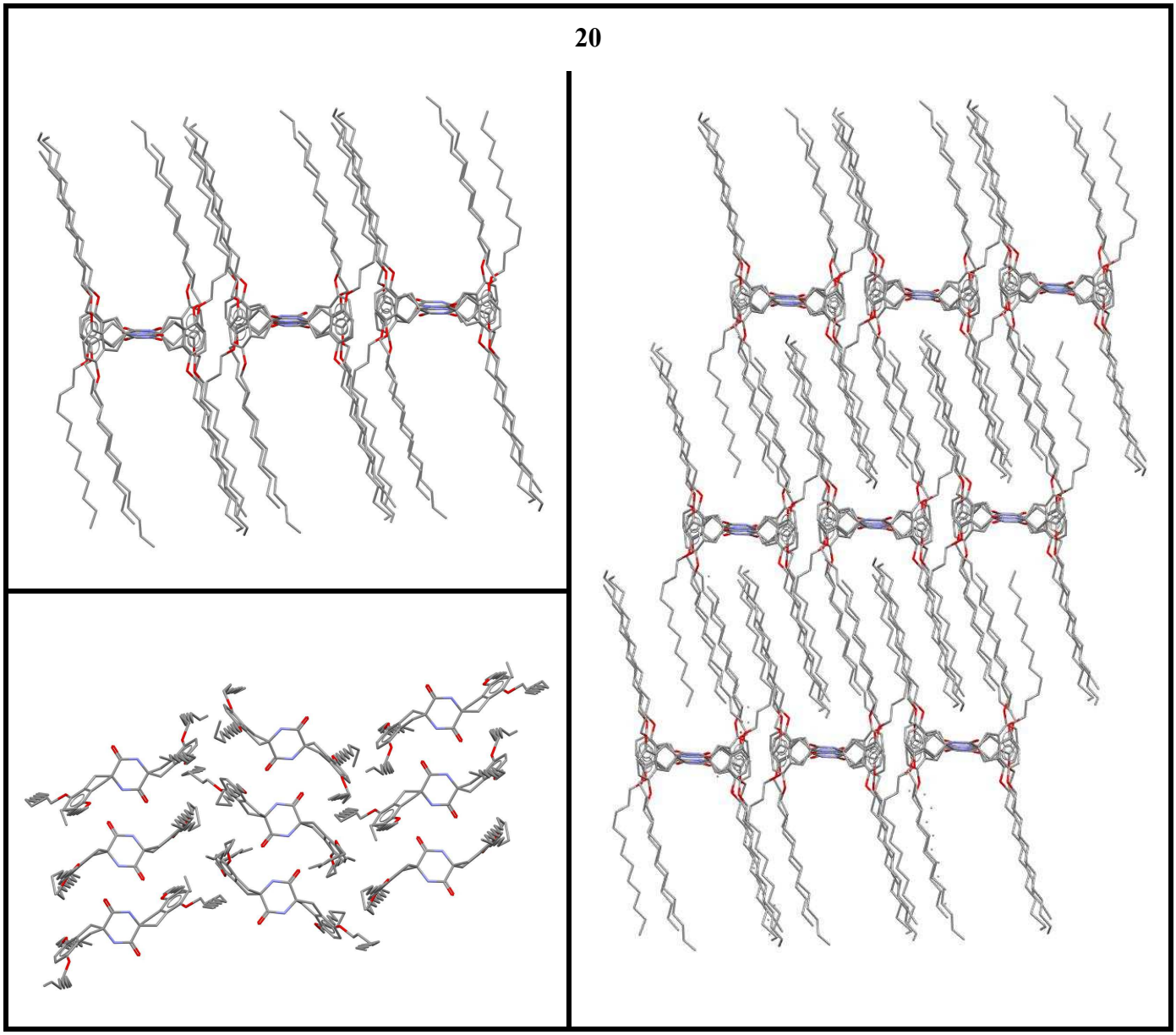

Figure 8. Crystal packing for piperazinedione **20**. Top left panel: a view of a sheet (nine molecules) formed by three LNTs viewed down the hydrogen-bonding axis. Bottom left panel: a view of the sheet perpendicular to the hydrogen-bonding axis. Right panel: a view of three sheets (27 molecules) down the hydrogen-bonding axis. Hydrogen atoms are omitted for clarity. Vertical neighbor tapes (VNTs) engage in van der Waals interactions through topographic complementarity (interdigitation of tails).

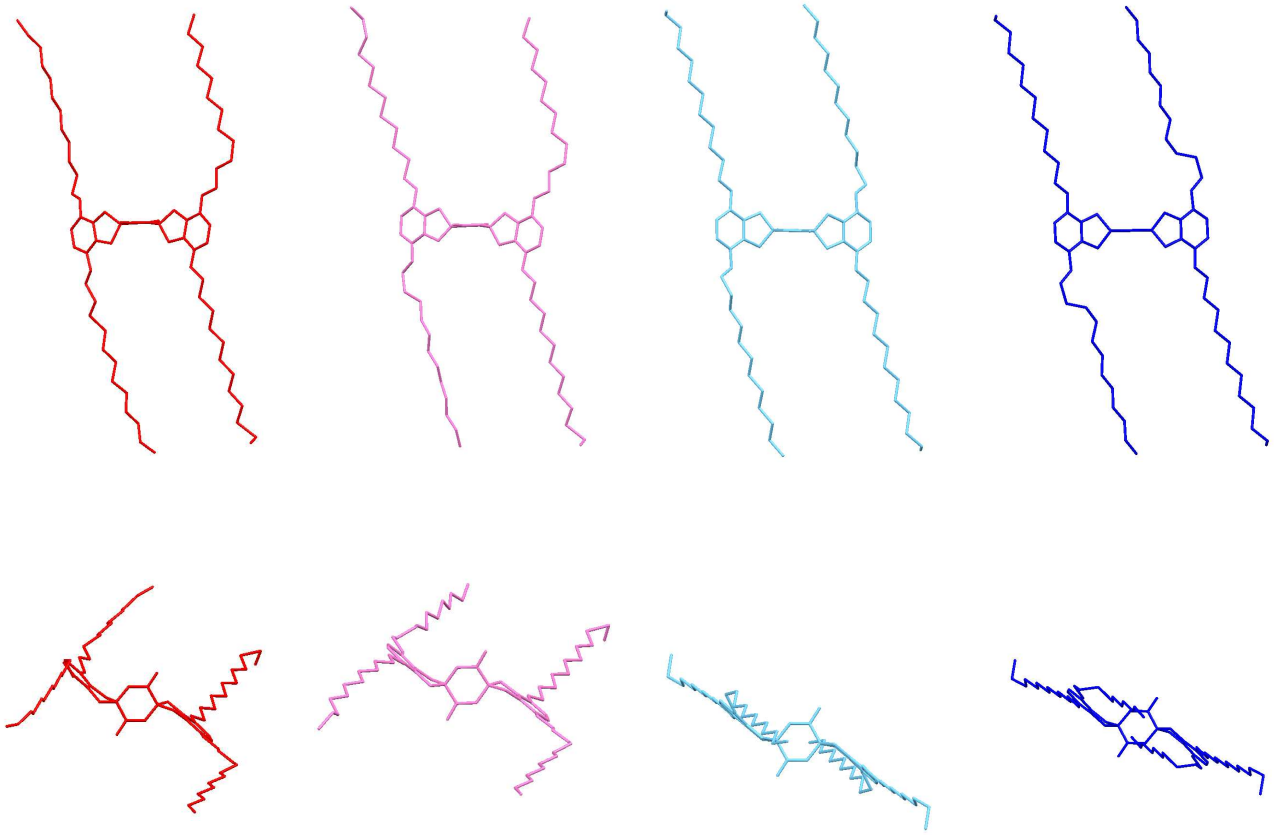

Conformer **20A** Conformer **20B** Conformer **20C** Conformer **20D**

Figure 9. Two views of conformers **20A-20D** found in the crystal structure of **20**. In these depictions, conformer **20A** is red, **20B** is lavender, **20C** is light blue, and **20D** is dark blue. Conformers *ent*-**20A** and *ent*-**20B** are not shown. *Top*: A view parallel to the plane of the piperazinedione ring. Bottom: A view perpendicular to the plane of the piperazinedione ring. The repeat pattern in a hydrogen bonded tape is …**20A**/**20B**::*ent*-**20A**/*ent*-**20B**::**20C**/**20D**…

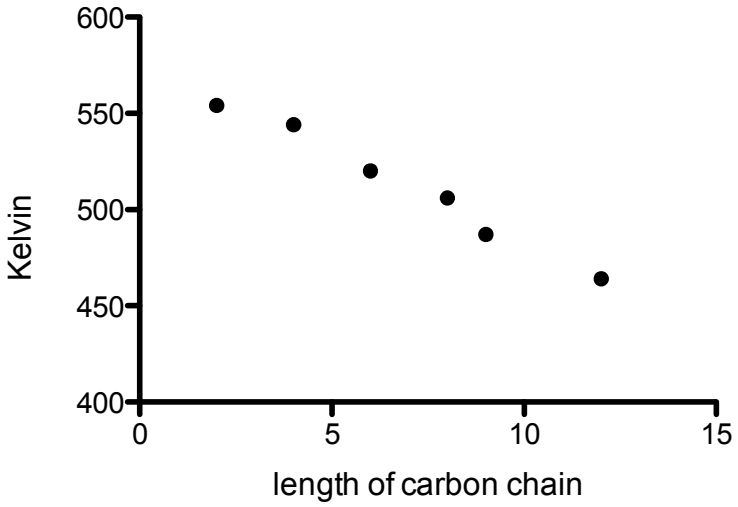

Figure 10. Graph of freezing point versus length of carbon chain for piperazinediones **15-20**. Compound **10** melted with substantial decomposition, and so its freezing temperature could not be determined. Sharp transitions were not observed for compound **21** over the range 375-475 K. The best-fit line has a correlation coefficient of 0.993.

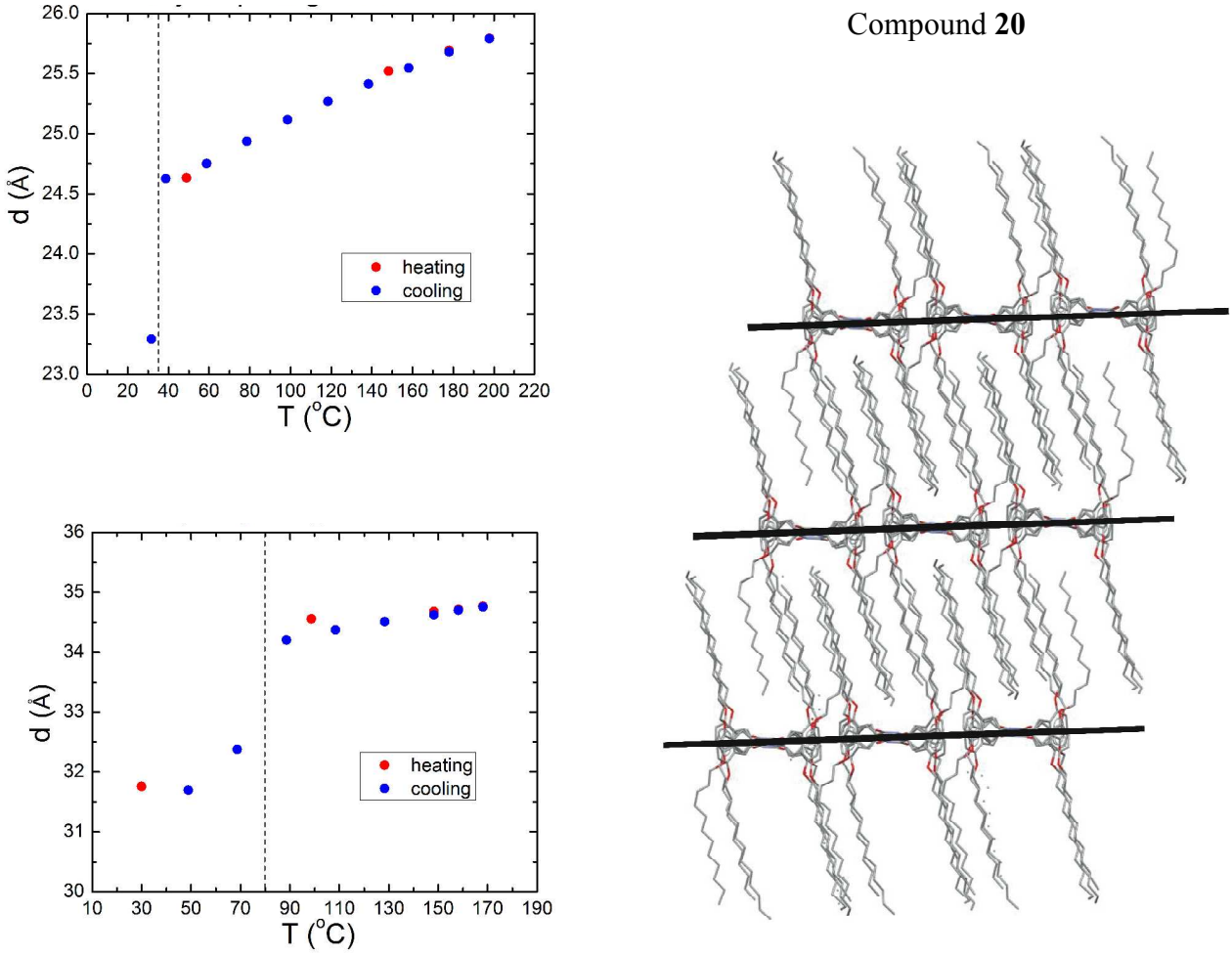

Figure 11. Changes in layer spacing with temperature for compounds **20** (top left) and **21** (bottom left) as determined by temperature-dependent X-ray analysis. The layer spacing undergoing change is presumed to be the distance between average planes of 2D sheets constructed from adjacent pentacyclic molecular cores, illustrated in cross section for compound **20** by the bars (right).

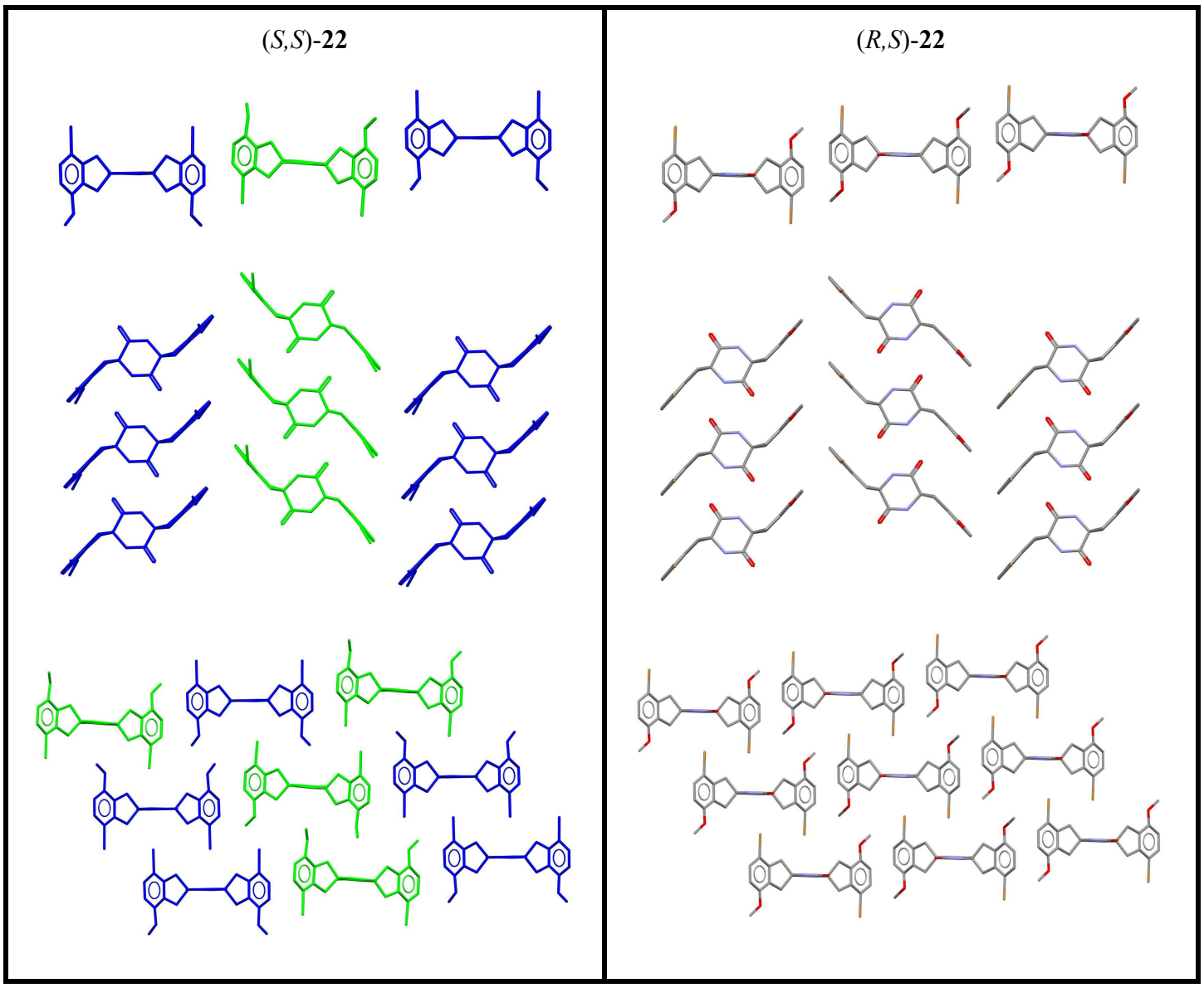

Figure 12. Crystal packing for piperazinediones (*S,S*)-**22** and (*R,S*)-**22**. Top of each panel: a view of a sheet (nine molecules) formed by three LNTs viewed down the hydrogen-bonding axis. Middle: a view of the sheet perpendicular to the hydrogen-bonding axis. Bottom: a view of three sheets (27 molecules) down the hydrogen-bonding axis. In the case of (*S,S*)-**22**, LNTs alternate between conformers A (blue) and B (green), while for VNTs the repeat pattern is …AABB... Hydrogen atoms are omitted for clarity.

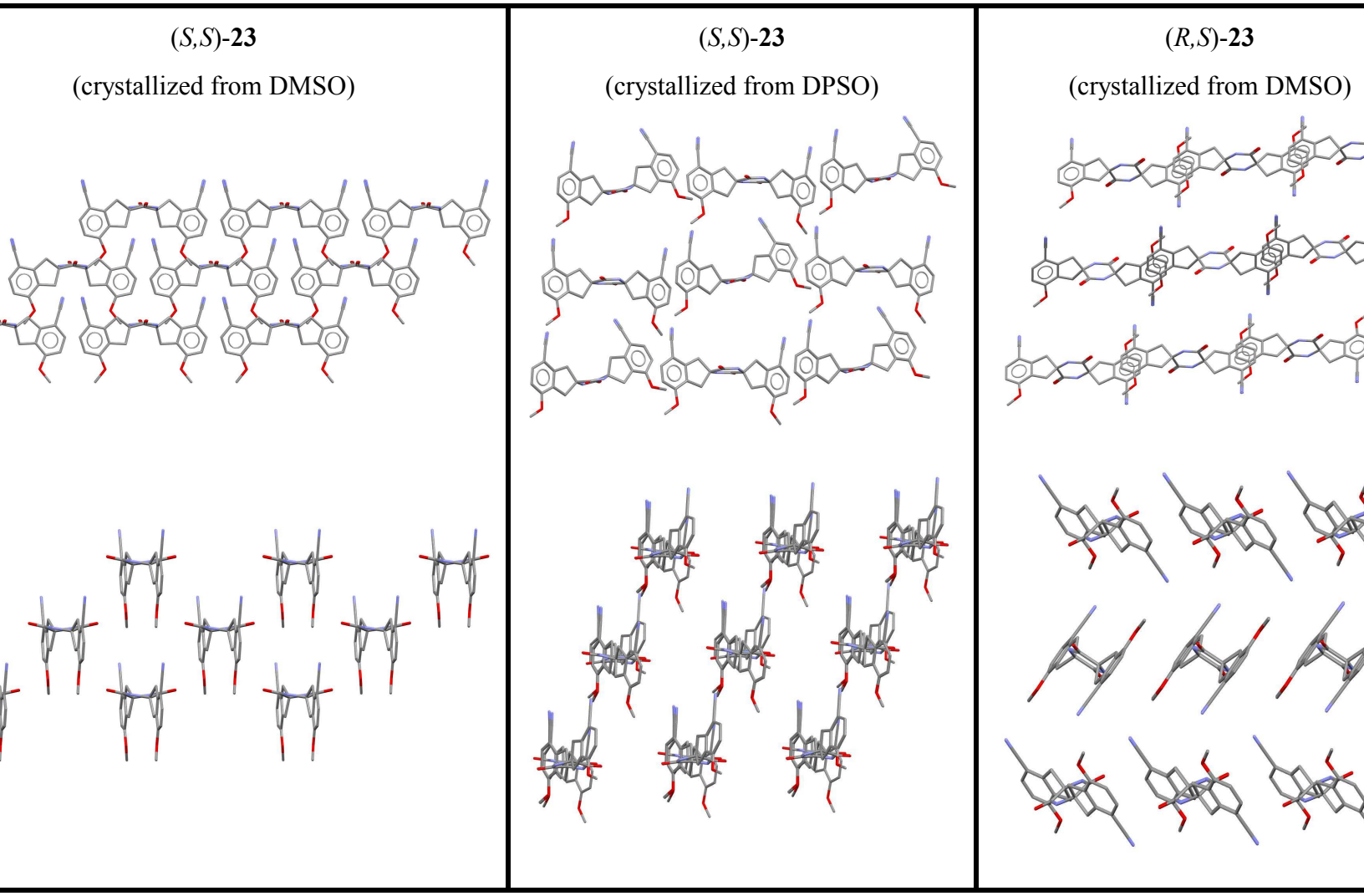

13. Crystal packing for piperazinediones (*S,S*)-**23** (crystallized from DMSO), (*S,S*)-**23** (crystallized from DPSO), and (*R,S*)-**23** (crystallized from DMSO) panel: a view of three sheets (27 molecules) approximately perpendicular to the arene rings. Bottom: a view approximately parallel to the arene rings. In molecules and hydrogen atoms are omitted for clarity.

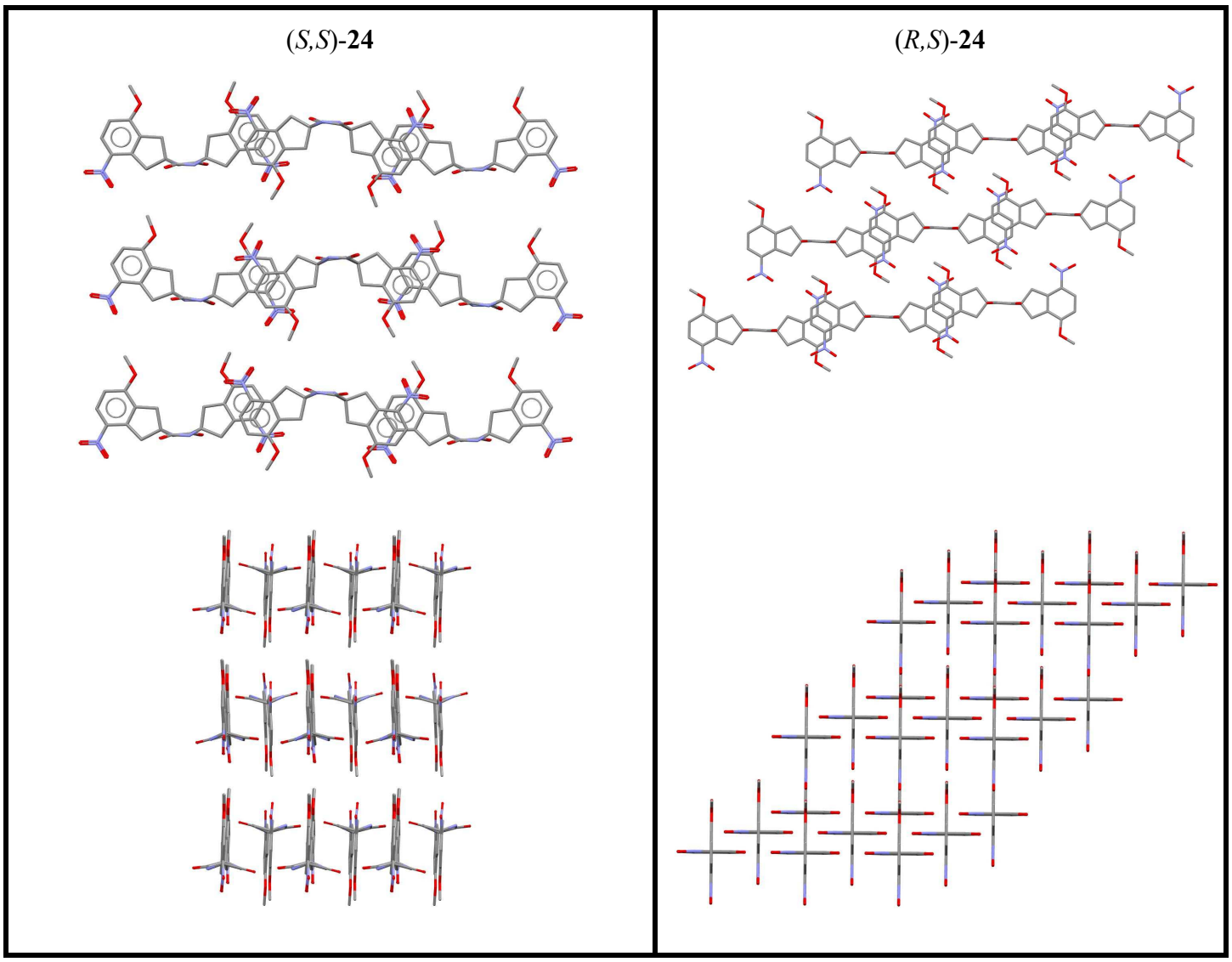

Figure 14. Crystal packing for piperazinediones (*S,S*)-**24** and (*R,S*)-**24**. Top of each panel: A view of three sheets (27 molecules) parallel to the hydrogen bonding axis. Bottom: A view perpendicular to the hydrogen bonding axis. Included solvent molecules (in the case of (*S,S*)-**24**) and hydrogen atoms are omitted for clarity.

(*R,S*)-**25**, (*S,S*)-**26**, and (*S,S*)-**27**

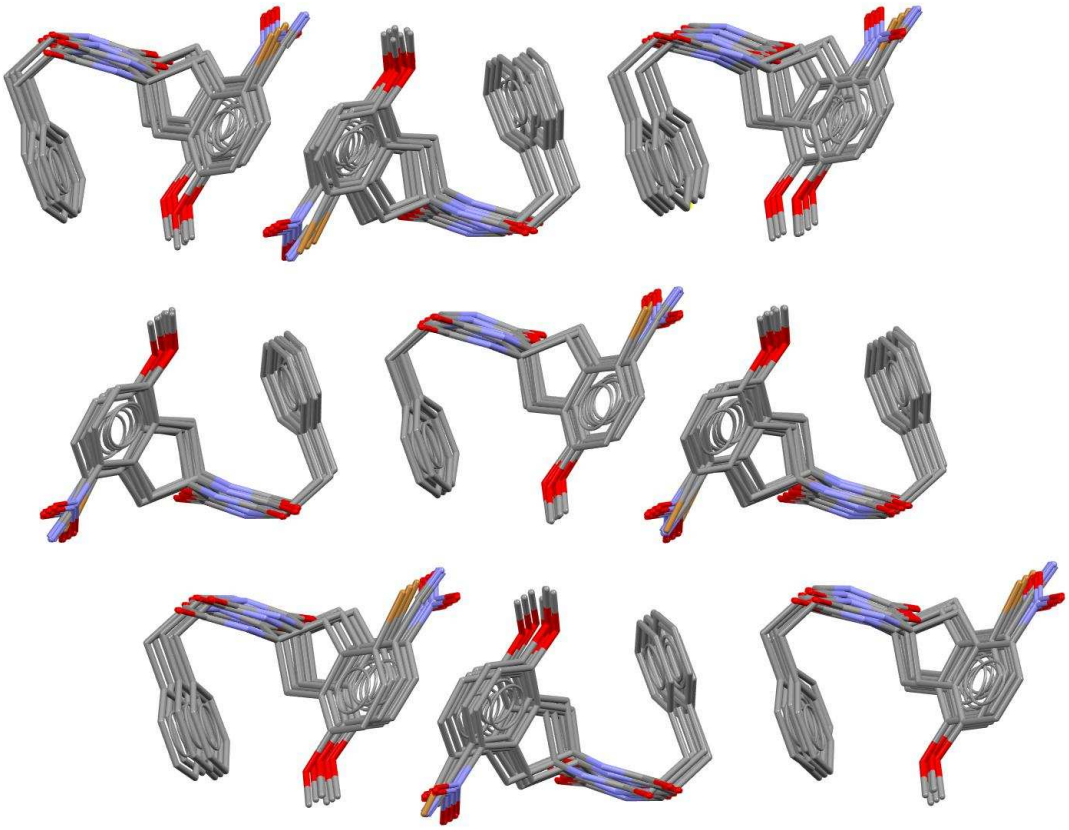

Figure 15. Overlay of the crystal packing of piperazinediones (*R,S*)-**25**, (*S,S*)-**26**, and (*S,S*)-**27**. This view is of three sheets (27 molecules) of each compound parallel to the hydrogen bonding axis. Hydrogen atoms are omitted for clarity.

Author Biography

Eugene A. Mash received Bachelors degrees in Chemistry and Biology from the University of California at Irvine in 1975 and a Ph. D. in Chemistry from the University of Utah in 1980 for work with Professor C. Dale Poulter on the mechanism of biological prenyltransfer. He received an NIH postdoctoral fellowship and worked on a chemical synthesis of saframycin B under the sponsorship of Professor E. J. Corey at Harvard University. In 1983 he joined the faculty of the University of Arizona where he is currently Professor of Chemistry and Biochemistry. Mash's early independent work focused on development of methods for asymmetric synthesis and application of his methods to natural product synthesis. Following a sabbatical spent at IBM's Almaden Research Center as the 1990-91 Paul J. Flory Fellow, Mash began to apply organic synthesis to problems in other fields. His current research interests include organic crystal engineering and multivalency as it pertains to biomedical imaging and drug delivery.

Table of Contents entry

Piperazinediones **1** that incorporate three geometrically and chemically independent recognition elements can assemble predictably into a solid.